NASA TECHNICAL REPORT

NASA TR R-151

NASA TR R-151

A STUDY OF GUIDANCE TO REFERENCE TRAJECTORIES FOR LIFTING REENTRY AT SUPERCIRCULAR VELOCITY

by Rodney C. Wingrove

Ames Research Center
Moffett Field, Calif.

NATIONAL AERONAUTICS AND SPACE ADMINISTRATION • WASHINGTON, D. C. • DECEMBER 1963

A STUDY OF GUIDANCE TO REFERENCE TRAJECTORIES FOR LIFTING REENTRY AT SUPERCIRCULAR VELOCITY

By Rodney C. Wingrove

Ames Research Center
Moffett Field, Calif.

NATIONAL AERONAUTICS AND SPACE ADMINISTRATION

For sale by the Office of Technical Services, Department of Commerce, Washington, D.C. 20230 -- Price $1.75

NATIONAL AERONAUTICS AND SPACE ADMINISTRATION

TECHNICAL REPORT R-151

A STUDY OF GUIDANCE TO REFERENCE TRAJECTORIES FOR LIFTING REENTRY AT SUPERCIRCULAR VELOCITY

By Rodney C. Wingrove

SUMMARY

This report presents an analysis of the guidance of lifting vehicles onto a reference trajectory during atmosphere entry. Various reference trajectories and various input quantities to govern lift variations are considered. A guidance method is developed which uses the four-state variables of a trajectory as follows: Velocity is made the independent variable and the errors in the rate of climb, acceleration, and range relative to the reference govern the lift. A linearized form of the motion equations is used to show that this method represents a third-order control system. First- and second-order terms (rate-of-climb and acceleration inputs) are shown to determine the entry corridor depth by stabilizing the trajectory so that the vehicle does not skip out of the atmosphere or does not exceed a specified acceleration limit. The destabilizing effect that range input (the third-order control term) can have is illustrated and the results indicate that a low value of range input gain must be used at the high supercircular velocities while larger values can be used at lower velocities.

The usable corridor depth and range capability with this guidance system are presented for a lifting capsule ($L/D = 0.5$) entering the atmosphere at a velocity 40 percent above local circular. The results show an attainable downrange increment of about 1,000 miles within a 25-mile entry corridor and 2,000 miles within a 10-mile corridor when a moderate range input gain is used only at velocities below local circular. The range increment is increased to about 3,000 miles within a 25-mile corridor and 4,000 miles within a 10-mile corridor when, in addition, a small range input gain is used above circular velocity.

INTRODUCTION

Current and future space-flight projects require the development of entry guidance methods applicable to vehicles entering the Earth's atmosphere at supercircular velocities. These methods must guide the vehicle to a predetermined destination and insure that acceleration and heating limits are not exceeded. Various entry guidance and control methods have been considered (e.g., refs. 1 through 11). Although these studies present solutions to the reentry guidance problem, they do not analyze in detail

how the control parameters influence the reentry guidance system. It is the purpose of this report to demonstrate, by means of control system analysis techniques, the influence of various control parameters upon the trajectory motion (see also ref. 12). A simple guidance technique based on a reference trajectory and moderate lift variations will be developed from these factors, and a linearized form of the entry motion equations will be used to describe mathematically the trajectory dynamics.

These guidance methods will be applied to a vehicle with a maximum L/D of 0.5 entering the earth's atmosphere at a velocity 40 percent above local satellite velocity. As shown in references, such as 13 and 14, entries, beginning at supercircular velocity, require that the lift be controlled to prevent the vehicle from skipping out of the atmosphere or exceeding a given acceleration limit. Methods for controlling lift to satisfy these constraints and to reach a desired landing site will be considered. The effect of the reference trajectory on acceleration and skip-out boundaries and also on maximum range capability will be investigated.

NOTATION

A	horizontal acceleration, g units
A_T	resultant acceleration, $A\sqrt{1+\left(\frac{L}{D}\right)_o^2}$, g units
C_D	drag coefficient, $\frac{D}{(1/2)\rho V^2 S}$
D	drag force, lb
g	local gravitational acceleration, ft/sec^2
h	altitude, ft
$\dot{h}$	rate of climb, fps
K_1, K_2, K_3	gain constants
L	lift force, lb
m	mass of vehicle, slugs
r	distance from planet center, ft
R	downrange value along local great circle route in space, statute miles

S	surface area on which drag coefficient is based, ft^2
u	circumferential velocity component normal to radius vector, ft/sec
$\bar{u}$	dimensionless ratio, $\frac{u}{\text{circular orbital velocity}}$, $\frac{u}{\sqrt{gr}}$
V	resultant velocity, ft/sec
W	weight of vehicle, lb
Z	dimensionless function of $\bar{u}$ determined by equation (1) and appropriate boundary conditions, $\rho\bar{u}\left(\frac{C_D S}{2m}\right)\sqrt{\frac{r}{\beta}}$
Z'	first derivative with respect to $\bar{u}$
Z''	second derivative with respect to $\bar{u}$
β	atmospheric density decay parameter, ft^{-1}
γ	flight-path angle relative to local horizontal; positive for climb
ρ	atmosphere density, slugs/cu ft
φ	roll angle
ψ	lateral deflection angle
ζ	damping factor
ω_n	natural frequency, radians/unit of $\bar{u}$

Subscripts

ref	respect to reference trajectory
1	initial value
2	final value
o	value at $\varphi = 0$

METHOD OF ANALYSIS

In this section the motion equations programmed on the computer will first be stated. Then a linear form of these motion equations will be developed to illustrate control factors that influence the system response. These control factors will then be considered in choosing a suitable method for guiding to a reference trajectory.

Trajectory Equations

The analysis is based on analog computer solutions of Chapman's approximate equation of entry motions (ref. 15). This simplified equation aids in the recognition of factors important to trajectory control and allows simplified computer programming. Chapman's basic equation as used in this study is

$$\frac{d^2Z}{d\bar{u}^2} - \frac{1}{\bar{u}}\frac{dZ}{d\bar{u}} + \frac{Z}{\bar{u}^2} - \frac{1 - \bar{u}^2}{\bar{u}^2 Z} + \frac{\sqrt{\beta r}\,(L/D)}{\bar{u}} = 0 \tag{1}$$

A block diagram of the analog computer set-up of this equation is illustrated in figure 1.

The initial conditions for solution of equation (1) on the analog computer are the initial entry conditions as follows:

$$\bar{u}_1 = \frac{V_1 \cos \gamma_1}{\sqrt{gr}} \tag{2}$$

$$Z_1 = \frac{-A_1}{\sqrt{\beta r}\,\bar{u}_1} \tag{3}$$

$$Z_1' = \left(\frac{dZ}{d\bar{u}}\right)_1 = \sqrt{\beta r} \sin \gamma_1 + \frac{Z_1}{\bar{u}_1} \tag{4}$$

The various quantities used by the control system are shown in figure 1 and are expressed as functions of Z, Z', and $\bar{u}$ as follows:

Rate of climb

$$\dot{h} = \sqrt{\frac{g}{\beta}}\,(\bar{u}Z' - Z), \text{ fps} \tag{5}$$

Horizontal acceleration

$$A = -\sqrt{\beta r}\,\bar{u}Z, \text{ g units} \tag{6}$$

Downrange

$$R = \frac{r}{5280\sqrt{\beta r}} \int_{\bar{u}_2}^{\bar{u}_1} \frac{1}{Z}\, d\bar{u}, \text{ statute miles} \tag{7}$$

The computation of crossrange normal to the plane of the trajectory was taken from Slye's approximation (ref. 16) as follows:

$$\text{Crossrange} = \frac{r}{5280\sqrt{\beta r}} \int_{\bar{u}_2}^{\bar{u}_1} \frac{\sin\psi}{Z}\, d\bar{u}, \text{ statute miles} \tag{8}$$

where

$$\frac{d\psi}{d\bar{u}} = -\frac{1}{\bar{u}}\left(\frac{L}{D}\right)_o \sin\varphi \tag{9}$$

These equations apply to any planetary atmosphere. In this study the particular constants for the earth are $\sqrt{\beta r} = 30$, $\sqrt{gr} = 25{,}800$ fps, and $r = 2.215 \times 10^7$ ft (4,000 miles).

The accuracy of Chapman's Z function method has been established by comparison with a more exact numerical calculation (refs. 2, 13, 15). The limitations of the Z function method are described in detail in reference 15, but are outlined here for convenience:

1. Drag during entry must be large enough that $dr/r \ll du/u$. For a first approximation, this is the case for reentry bodies at altitudes up to approximately 300,000 feet.

2. Atmosphere density varies exponentially with altitude.

3. The entry is sufficiently shallow that $\cos\gamma = 1$, $\sin\gamma = \gamma$; $L/D \tan\gamma$ and $\tan^2\gamma$ can be disregarded compared with unity.

4. The earth is cylindrical and nonrotating. (The "flat earth" approximation has been shown in reference 16 to be very good up to 1,000 miles crossrange.)

5. Vehicle m/C_DS is a constant. These results therefore apply to those vehicle configurations in which there are essentially no drag changes with lift, as in the case where roll angle is used to control the component of normal force in the vertical plane.

Linearized Entry Equations

Equation (1) is nonlinear and therefore does not allow the use of standard control system analysis techniques. To use linear analysis techniques and obtain an approximate description of the entry trajectory motions, a linearized trajectory equation was derived from the Chapman equation. This derivation is presented in the appendix. The linearized equation will be used throughout this report to describe, in an approximate fashion, the effect of various control quantities on the trajectory motions. The linearized equation, taken from the appendix, corresponding to equation (1) is:

$$\Delta Z'' - \frac{1}{\bar{u}} \Delta Z' + \frac{\beta r(1 - \bar{u}^2)}{A_{ref}^2} \Delta Z = \frac{-\sqrt{\beta r}\, \Delta(L/D)}{\bar{u}}$$

The Δ terms represent linear deviations from the reference trajectory.

This linear equation can be used to aid in the recognition of factors important in trajectory control. The following simplified sketch illustrates these factors. The equation of motion is seen to be a second-order-differential equation in either altitude, temperature, or acceleration

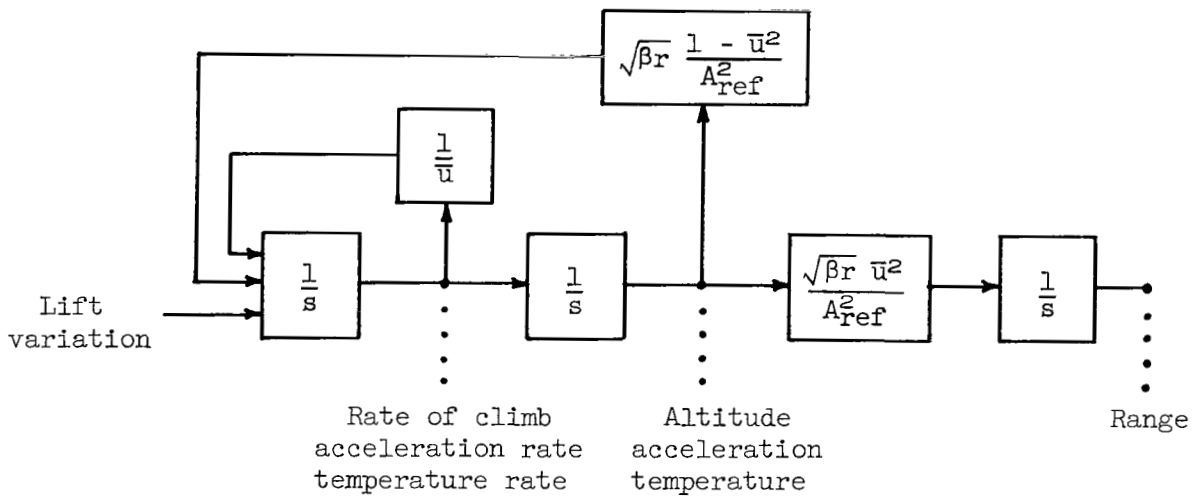

along the trajectory. (Temperature is not used for the control systems considered in this report (see ref. 1).) It is important to examine the loops inherent in the motion equation shown in the sketch. The upper loop, $\sqrt{\beta r}\,(1 - \bar{u}^2)/A_{ref}^2$, corresponds to the spring constant of the second-order differential equation, and, therefore, it determines the natural frequency of the trajectory oscillations. This loop is stabilizing when velocity, $\bar{u}$, is less than 1 (local circular velocity), but it is destabilizing when velocity is greater than 1. The lower loop, $1/\bar{u}$, is a first-order damping term that adds damping to the trajectory oscillations.

This simplified representation of the dynamics gives some insight into the terms a lift control system should incorporate. For instance, lift variation controlled by range measurements represents a third-order function with respect to velocity. It can be reasoned that this system like any other classical third-order system of control, needs first- and second-order feedback terms for good dynamic response. The first-order term in this case can be represented by the rate of change of altitude, acceleration, or temperature and the second-order term can be represented by the value of altitude, acceleration, or temperature. It appears that simple entry control techniques can be conceived from these system dynamics As an example, the control technique described in the following section will be used in this report to illustrate these factors.

Control Method

The control technique used in this report is the method of guiding to a reference trajectory. As pointed out previously, the target motion is described by the four-state variables, velocity, $\bar{u}$, rate of change of altitude, $\dot{h}$, acceleration, A, and range, R. In this investigation, velocity, $\bar{u}$, is the independent variable, and the errors in $\dot{h}$, A, and R away from the reference trajectory are used to govern lift in the following manner:

$$L/D = (L/D)_{ref} + K_1\Delta\dot{h} + K_2\Delta A + K_3\Delta R$$

where $(L/D)_{ref}$ is the lift-drag ratio function used to generate the reference trajectory, and the error quantities $\Delta\dot{h}$, ΔA, and ΔR are the deviations of the measured variables from their calculated values on the reference trajectory at the same velocity, $\bar{u}$. Figure 2 is a block diagram which illustrates this control method. It is important to note from the previous section that this control method uses the difference in range from that of the reference trajectory as the third-order feedback term, with the errors in acceleration and in rate of climb used as second- and first-order feedback terms.

The reference trajectories in this report are obtained by the following L/D control function:

$$(L/D)_{ref} = K_1\dot{h}_{ref}$$

The choice of this particular L/D function to describe the reference trajectory will be discussed fully in the text; this function simplifies the full control equation to:

$$L/D = K_1\dot{h} + K_2\Delta A + K_3\Delta R$$

In subsequent sections of this report the trajectory dynamics that result from control of L/D by various combinations of the three terms in this equation will be considered in detail.

Simulation Details

Equation (1) describes the reentry trajectory in terms of the independent variable $\bar{u}$ instead of the more conventional independent variable t (time). Since an electronic analog computer was used to solve the trajectory equation, it was necessary to define a relationship between the rate of integration of the computer and the independent variable $d\bar{u}$. An integration rate was chosen in which one second was equal to a $d\bar{u}$ of -0.1. The initial conditions used were $\bar{u} = 1.4$ and $Z = 0.004$, corresponding to an entrance velocity of about 36,000 fps and an initial acceleration of 0.17g. The L/D limits for the vehicle were chosen as ± 0.5.

To obtain the state variable of a particular reference trajectory, a second solution of equation (1) was run simultaneously with the reference entrance conditions and a reference L/D program. Hence, during the simulated run, the reference value of a given feedback signal was available for comparison with the actual value, thereby giving the error signal to be used in feedback control.

RESULTS AND DISCUSSION

Chapman (ref. 13) has shown that a vehicle returning to the Earth at supercircular velocity must be guided into a safe entry corridor. Figure 3 illustrates the corridor depth which is the distance between the conic perigee of the overshoot boundary (beyond which the vehicle will skip out of the atmosphere) and the undershoot boundary (beyond which the vehicle will exceed its specified acceleration limit). An alternate way to describe this safe entry corridor is in terms of the initial entrance angles for the two boundary trajectories. In this study the initial entrance angle is used to specify the trajectory.

The use of first- and second-order inputs ($\dot{h}$, and A) to control the trajectory over a satisfactory corridor depth will first be discussed. Then the effect of third-order range inputs and the manner in which they should be employed will be discussed. Maximum values of downrange and crossrange available when the reference trajectory control method is used will be shown.

Trajectory Stabilization

Trajectory stabilization is here defined as the damping of vehicle motion about a specified design trajectory. It should be noted that the limits of permissible trajectory oscillation were established as those points at which the vehicle will either skip back out of the atmosphere ($A \approx -0.05g$) or exceed a given acceleration limit ($A = -10g$ in most given examples).

Rate damping.- The control function considered for rate damping of the entry trajectory is

$$L/D = K_1\dot{h}$$

Figure 4 illustrates typical reentry trajectories in which L/D is controlled as a function of the rate of climb. The plot of acceleration versus velocity (fig. 4(a)) was obtained from the solution of equation (1). The corresponding range, command L/D, and altitude variations are presented in figures 4(b), 4(c), and 4(d). In the computation of altitude a drag loading W/C_DS of 48 psf has been used.

This figure indicates the entrance angle limits within which a safe entry can be made. An entrance angle of -3.97° will cause the vehicle to skip out of the atmosphere. This skip-out entrance angle is considerably greater than the skip-out entrance angle of $\gamma = -2.2^\circ$, which results when L/D is held constant at -0.5. The steepest possible entrance angle ($\gamma = -6.0^\circ$ in the figure) is determined by the maximum acceleration limit of -10g. This realistic acceleration limit for humans (ref. 17) has been used in this report in defining usable corridor depths.

The trajectories illustrated in figure 4 have a given value of $\dot{h}$ feedback gain, K_1. Control gain affects the entrance angle limits as shown in figure 5. It should be noted that the entrance angle is plotted to a nonlinear scale so that corridor depth in miles may be obtained by linear interpolation. It is seen that with zero feedback gain, and thus L/D = 0, there is an available corridor depth of about 8 miles. With infinite feedback gain (i.e., L/D = +0.5 when $\dot{h}$ is negative; L/D = -0.5 when $\dot{h}$ is positive), the available corridor depth is about 30 miles out of 40 miles available to the vehicle if controlled in an optimum manner.

As mentioned previously the design reference trajectories are for the L/D function proportional to rate of climb (i.e., $L/D_{ref} = K_1\dot{h}_{ref}$). Five such reference trajectories which differ only in initial entrance angles are shown in figure 6; the rate-of-climb gain, K_1, is -0.001/fps. It is seen in figure 6 that L/D is maximum during the initial portion of the trajectory and the L/D varies to stabilize the trajectory. Near the end of the trajectory the L/D is about one-half the maximum positive value resulting in a trajectory near the middle of the vehicle's subcircular maneuvering capability.

Control system with acceleration inputs.- The use of acceleration error in controlling L/D was investigated for the reference trajectories of figure 6. The control function for L/D was

$$L/D = (L/D)_{ref} + K_2\Delta A$$

where ΔA is the difference between the actual acceleration and the reference trajectory acceleration at a given velocity, and $(L/D)_{ref}$ is the reference L/D value at a given velocity along the trajectory. Figure 7 illustrates the effect of K_2 on the acceleration error for a

typical controlled trajectory. The actual acceleration is seen to oscillate about the reference value. The characteristics of the motion resulting from L/D correction as a function of acceleration errors can be approximated by linearized analysis (appendix) as follows:

Damping

$$2\zeta\omega_n \approx \frac{1}{\bar{u}}, \frac{\text{radians}}{\text{unit of } \bar{u}}$$

Natural frequency

$$\omega_n^2 \approx 900\left(\frac{1 - \bar{u}^2}{A_{ref}^2} - K_2\right), \left(\frac{\text{radians}}{\text{unit of } \bar{u}}\right)^2$$

This linear analysis does not take account of the L/D = ±0.5 limit that is imposed; however, for small oscillations about the reference trajectory, and for a finite value of K_2, the linearized equation gives a good description of the motion (see appendix). From the linear analysis the acceleration feedback term is shown to be analogous to a spring restoring term in a classical second-order system. As shown in figure 7, the frequency of oscillation increases with the gain, K_2. The oscillation frequency shown in this figure for trajectory with no acceleration control ($K_2 = 0$) is the inherent natural frequency of entry motion and can be predicted from the linearized equations.

The use of acceleration error in controlling to reference trajectories 4 and 2 is shown in figures 8 and 9, respectively. Control to trajectory 4 (fig. 8) keeps the vehicle within the atmosphere for any entrance angle steeper than the -3.63° skip-out limit. In contrast, acceleration error control to trajectory 2 (fig. 9) results in skip-out with entrance angles steeper than about -4.4°. For trajectory 2 there is only a small range of entrance angles (from -3.6° to -4.4°) for which the controlled trajectory will not skip-out. There is skip-out at steeper entrance angles because this design trajectory has a low acceleration profile. In other words, with a controlled trajectory which passes up through this design trajectory there is little margin between the design trajectory acceleration and zero acceleration at which the vehicle skips out.

The corridor limits with each of the five reference trajectories are shown in figure 10 as a function of peak acceleration. These corridor limits are compared with the idealized corridor limits attainable with a vehicle of L/D = ±0.5 capability. The entrance angle at which skip-out will occur when controlling to each of the various design trajectories is also shown in this figure. Two values of feedback gain, $K_2 = -\infty$ and $K_2 = -0.33/g$ were investigated. With infinite feedback gain, (fig. 10(a)), the vehicle could be controlled to trajectories 4 and 5, and remain within the atmosphere for a wide range of entrance angles. For trajectories 3 and 2 there is only a small range of entrance angles for which the vehicle

would stay within the atmosphere; and with trajectory 1 it would remain in the atmosphere only at the design entrance angle.

With the smaller feedback gain (fig. 10(b)), the entrance angle limits are small for trajectories 3 and 2, and again, for reference trajectory 1, the vehicle would stay within the atmosphere only at the design entrance angle.

It is apparent that control to a reference trajectory with acceleration error alone controlling L/D is not satisfactory because of the oscillatory nature of the controlled trajectory and the rather limited range of possible entrance angles for some reference trajectories.

Acceleration and rate-of-climb inputs.- It can be reasoned that the addition of rate-of-climb inputs might damp undesired oscillations and thus provide smoother control of the trajectory. The control of L/D by acceleration in combination with rate of climb was used in the following manner:

$$L/D = (L/D)_{ref} + K_1\Delta\dot{h} + K_2\Delta A$$

Figure 11 illustrates the results for this control system. It is particularly evident in this figure that rate of climb damps the trajectory. With rate-of-climb feedback gain on the order of -0.001/fps, the trajectory motion is damped, with a small overshoot, by the time the vehicle has reached circular velocity ($\bar{u} = 1$).

Again, the characteristics of this motion can be approximated by the linearized analysis in the appendix.

Damping

$$2\zeta\omega_n \approx \frac{1}{\bar{u}} - 25{,}800\ K_1,\ \frac{\text{radians}}{\text{unit of } \bar{u}}$$

Natural frequency

$$\omega_n^2 \approx 900\left(\frac{1 - \bar{u}^2}{A_{ref}^2} - K_2\right),\left(\frac{\text{radians}}{\text{unit of } \bar{u}}\right)^2$$

As an example, if values of $K_1 = -0.001$/fps, $K_2 = -0.33/g$, and $\bar{u} = 1$ are inserted in the simplified expressions, the computed damping is $\zeta = 0.78$. A comparison of this computed ζ with the corresponding curve in figure 11 shows good agreement. Thus it is felt that the linearized expressions of the appendix not only allow a qualitative consideration of the trajectory dynamics, but they also give a quantitative description of certain aspects of the trajectory dynamics.

The use of combined acceleration and rate-of-climb inputs was investigated with each of the five reference trajectories for entrance angles within the corridor. Typical results for the control to reference trajectory 2 is shown in figure 12. With the extreme entrance angles illustrated, the controlled response of the vehicle is such that it is damped onto the design trajectory by the time the vehicle's speed is below circular velocity.

The corridor limits with combined $\Delta\dot{h}$ and ΔA control to each of the five design trajectories are illustrated in figure 13, as a function of the peak acceleration. As in the previous case these corridor limits are compared with the idealized corridor limits attainable with a vehicle of $L/D = \pm 0.5$ capability. The entrance angle at which skip-out will occur when controlling to each of the various design trajectories is also shown in this figure. There is a trend in these data for the corridor depth to be narrower for the shallower design trajectories. For example, the 10g corridor depth of trajectory 1 is about 33 miles compared with 37 miles for trajectory 5.

In figure 14 is a comparison of the usable corridor depths as a function of the allowable peak acceleration for the control combinations that have been discussed thus far. These data are for the control gain values that give maximum corridor depth. Acceleration inputs alone allow use of almost all the available corridor depth for maximum acceleration limits above about 7g. For acceleration design limits below 7g, the addition of rate of climb adds to the available corridor depth. Using rate of climb results in an available corridor depth of about 10 miles less than the maximum available, independent of the acceleration limit. In addition to these considerations of corridor depth, it should be restated that only with the combined rate-of-climb and acceleration inputs will the controlled trajectory damp onto a design reference trajectory over a wide range of entrance conditions.

Range Control

The full L/D control equation, which includes range input, is the following:

$$L/D = (L/D)_{ref} + K_1\Delta\dot{h} + K_2\Delta A + K_3\Delta R$$

The range error term, ΔR, is the difference between actual range to go and the reference range to go as a function of the velocity along the trajectory. By driving this error to zero at the end of the trajectory the vehicle will reach the desired destination. The terms, $K_1\Delta\dot{h}$ and $K_2\Delta A$, are identical to those considered in the previous section.

Effect of gains.- The effect of range input gain, K_3, is shown in figure 15 for a given initial range error. The use of too small an input gain will not eliminate the range error by the end of the trajectory.

On the other hand, too large a range input gain will overcontrol the vehicle and cause it to skip out, as illustrated in figure 15 for $K_3 = 0.01/\text{mile}$. The choice of a proper degree of range control is a compromise between these two effects.

The effect of the other feedback gains (K_1 and K_2) on range control is shown in figure 16. As pointed out previously, with range input the control of L/D is essentially a third-order system. As with any third-order control system, it was found that including the two inner loop terms (i.e., $\Delta\dot{h}$ and ΔA) allows a higher outer loop gain for tight control. The manner in which the values of K_1, K_2, and K_3 will shape the control system response is shown in figures 15 and 16.

In order to gain a better understanding of these effects, the linearized expression for the trajectory motions can be used. From the appendix the linearized motion equation at local points along the trajectory can be obtained in the following manner for the control quantities considered herein:

$$s^3 + \left(\frac{1}{\bar{u}} - 25{,}800\ K_1\right) s^2 + 900 \left(\frac{1 - \bar{u}^2}{A_{ref}^2} - K_2\right) s + \frac{3.6 \times 10^6\ \bar{u}}{A_{ref}^2} K_3 = 0$$

This is a linear third-order equation and the standard methods for analyzing this type of equation can be used to gain insight into the control dynamics. One simple approach in looking at the dynamics is to consider the highest values of range input gain (K_3) that can be used without causing the motion to become unstable. The stability criterion (i.e., Routh's method) is that the system will be unstable when

$$K_3 > \frac{\left(\frac{1 - \bar{u}^2}{A_{ref}^2} - K_2\right)\left(\frac{1}{\bar{u}} - 25{,}800\ K_1\right)}{4000\ \bar{u}} A_{ref}^2$$

The above expression can be used to determine the upper limit on K_3 and can be used to observe the qualitative interaction of K_1, K_2, K_3, and $\bar{u}$ on trajectory stability. The addition of K_2 in the term,

$$\left(\frac{1 - \bar{u}^2}{A_{ref}^2} - K_2\right)$$

provides a stable response above circular velocity. Increasing the magnitude of K_1 and K_2 will allow the upper limit on K_3 to increase and it is important to note that the upper limit on K_3 will increase as $\bar{u}$ decreases.

To maximize the available range capability and drive the range error to zero at the end of the trajectory, it is desirable to have as large a value of range input gain K_3 and still maintain a margin of system

stability. From stability considerations this value of gain must be low at high velocities (i.e., $\bar{u} > 1$) and can only be increased at lower velocities (i.e., $u < 1$).

Range limits.- The effect of the range input, $K_3\Delta R$, to the control system will become more pronounced as the value of range error, ΔR, at entrance is increased. This is illustrated in figure 17 with reference trajectory 3 for a constant input gain K_3 and for various values of initial range error. A skip-out is shown for an initial range error of 175 miles. This skip-out is due to the high value of range input $K_3\Delta R$ causing an L/D command which overpowers the trajectory control terms, $K_1\Delta\dot{h}$ and $K_2\Delta A$. Diving below the design trajectory, in order to shorten range, incurs the hazard of exceeding the acceleration limit as illustrated in figure 17. An initial range-to-go value of about 400 miles less than the reference range to go can be seen to call for deceleration values greater than 9g.

For a constant gain control system, the position along the trajectory at which the range input is commenced will alter the permissible initial range errors. Figure 18 presents the initial range error limits as a function of the velocity at which the range input term is added to the trajectory control terms. As mentioned above, when range input is added at supercircular velocities, the range error is limited by the skip-out and deceleration limits. At a speed just below satellite velocity, the vehicle cannot skip out and the maximum L/D available can be used for range control.

These data in figure 18 are for reference trajectory 3. The range increment between the maximum and minimum initial range error limits from figure 18 is compared in figure 19 with those permissible when reference trajectories 1, 2, and 4 are used. The greatest range is obtained with the shallow entrance trajectory (No. 1) and is achieved when the constant gain range error is added to the control system at just below circular velocity. With trajectory 4 there is very little change in range capability regardless of the velocity at which range control is started because of the steeper descent and correspondingly shorter total range traveled. From these data for constant range control gains, it is inferred that a greater degree of range control is possible for shallow entrance trajectories.

The maximum downrange limit considered in this report is for the trajectory remaining within the "sensible atmosphere," usually referred to as a "direct descent" entry (refs. 18 and 19). With this limit, the maximum achievable range becomes a function of the minimum allowable acceleration which the vehicle encounters during entry. The maximum range limit for "direct descent" entries can be approximated from equilibrium glide at maximum L/D as shown in figure 20. The acceleration along this trajectory can be substituted into the general range equation

$$R = \frac{r}{5280} \int_{\bar{u}_2}^{\bar{u}_1} \frac{\bar{u}\, d\bar{u}}{-A} \qquad (10)$$

to give the approximate maximum range

$$R_{max} = \frac{r(L/D)}{5280}\left[1 + \frac{1}{2}\ln\frac{-(1 - \bar{u}_1^2)(1 - \bar{u}_2^2)}{(L/D)^2(A_{min})^2}\right] \qquad (11)$$

This range value is strongly affected by the minimum acceleration the vehicle will encounter. For example, the maximum range is 9,300 miles for a minimum acceleration of -0.05g ($h_{max} \approx 290{,}000$ ft), but only 4,700 miles for -0.5g ($h_{max} \approx 250{,}000$ ft). This maximum range is compared in figure 21 with the maximum range obtainable with the various reference trajectories using constant gain range control and keeping within $A_{min} = -0.05g$. The velocity at which range control is started for each of the trajectories corresponds to those values shown in figure 19 to give maximum range. Maximum ranges are between 3,000 miles (for trajectory 4) and 7,000 miles (for trajectory 1) whereas 9,300 miles range could conceivably be obtained near equilibrium glide. It will be noted that practical maximum range decreases with steeper entrance angles because a large amount of vehicle kinetic energy is lost during the initial steep dive into the atmosphere.

The minimum range obtainable during entry is primarily a function of the allowable acceleration limit. The absolute minimum range for constant acceleration can be obtained from equation (10) as

$$R_{min} = \frac{r}{5280}\left(\frac{\bar{u}_2^2 - \bar{u}_1^2}{2A_{max}}\right) \qquad (12)$$

From the initial velocity of $\bar{u}_1 = 1.4$, the absolute minimum range is about 400 miles for a -10g constant acceleration and 800 miles for a constant -5g acceleration. Actual trajectories are not characterized by a constant acceleration value, but the aforementioned minimum range equation gives an indication of the absolute limits to be expected. This absolute minimum range is compared in figure 22 with the minimum ranges obtained for the various design trajectories. The minimum ranges obtained are from 1,000 to 1,500 miles for trajectory 4 and from 2,000 to 5,500 miles for trajectory 1, compared to an absolute minimum range limit of about 400 miles.

As pointed out previously, stability considerations dictate that the range gain should be low at the higher velocities and high at lower velocities. To obtain more of the available range during entry, a two-step range gain was considered in the following manner:

$$L/D = (L/D)_{ref} + K_1\Delta\dot{h} + K_2\Delta A$$

$$+ K_3\Delta R \qquad K_3 = 0 \text{ when } \bar{u} \gtrsim 1$$

$$+ K_3'\Delta R \qquad K_3' = 0 \text{ when } \bar{u} \lesssim 1$$

The subcircular range term is the same as that shown previously. The supercircular range term, $K_3'\Delta R$, was investigated for both a small gain constant (K_3') and an upper limit on ($K_3'\Delta R$) so that the range term would not override the other terms and cause the vehicle to skip out. Figure 23 illustrates the control for maximum range with and without the two-step range gain. A value of $K_3' = 0.0008$/mile and an upper limit on the range term of $K_3'\Delta R = 0.1$ for $\bar{u}$ above 0.98 were found to be satisfactory with this trajectory. This two-step control-gain system extends the maximum range from 4,500 miles to 5,800 miles. To get this range extension, the trajectory is flown closer to the skip-out boundary during the supercircular portion with no increase in the maximum peak altitude.

The minimum range is presented in figure 24 both with and without the two-step range gain. The minimum range is reduced from about 2,100 miles to 1,200 miles by the two-step system. This change in minimum range was achieved by flying a profile of higher acceleration at supercircular velocity with no marked increase in the maximum value of acceleration.

The results for trajectory 2 shown in figure 25 illustrate the range capability that can be obtained in this manner. The two-step system provides a 500- to 2,000-mile reduction in minimum range. Futhermore, there is a large increase in maximum range for the small entry angles, but comparison with the idealized maximum range shows that the full capability is not achieved. The reason the ideal range is not obtained is that the control becomes sensitive near the ideal trajectory because of the proximity of the skip-out region. About 6 miles of corridor depth is lost by using the added range control term for range extension.

The range capability added by the two-step control gain system for trajectories 3 and 4 is very similar to that shown in figure 25 for trajectory 2. Two-step gain control was investigated for trajectory 1, but since this trajectory skips up to the edge of the atmosphere, it is very sensitive to control during the initial dive into the atmosphere. Because of this sensitivity problem, the second range control term ($K_3'\Delta R$) was not used with trajectory 1.

Crossrange capability.- In figure 26, the maximum crossrange capability is shown as a function of the velocity at which control is started for the various reference trajectories. In computing the maximum crossrange capability, it was assumed that the vehicle was trimmed at a constant value of $(L/D)_o = 0.5$ throughout the trajectory. The vehicle was rolled so the total lift vector was positioned to yield maximum crossrange capability while providing the lift required for downrange control. The roll command was made according to the following equation:

$$\text{command } \varphi = \pm\cos^{-1}\frac{\text{desired } (L/D)}{\text{trim } (L/D)_o}$$

The curves in figure 26 illustrate the important fact that for maximum crossrange, lateral control must start near the beginning of the trajectory. For entry at supercircular velocity, trajectory 1 which has the largest downrange capability also has the largest crossrange capability. At $\bar{u} = 1$ all the design trajectories have about ±200 miles of available crossrange which, as Slye (ref. 16) has shown, is typical of a vehicle with an $L/D = 0.5$ entering the atmosphere from circular velocity.

Attainable ground area.- The attainable ground area for two different corridors, and when the vehicle is controlled to design trajectory 2, is shown in figures 27(a) and 27(b). The conics in these figures represent the vacuum trajectories for the extreme entry angles at the boundaries of the corridor. The shaded area represents the ground area that can be reached from any entry angle within the corridor. In figure 27(a) with the 25-mile usable corridor for γ_1 between -4° and -6°, the attainable ground area is about 2,200 miles of downrange and ±250 to ±350 miles of crossrange. In figure 27(b) it can be seen that for an 11-mile corridor between $\gamma_1 = -4^\circ$ and -5°, there are 3,900 miles of downrange and ±250 to ±550 miles of crossrange available. The maximum acceleration encountered with the 25-mile corridor is 10g as compared with about 6g for the 11-mile corridor. These data illustrate the trade off between the specified corridor depth and attainable ground area; the largest ground area can be attained if the entry can be made within the smallest specified corridor.

A comparison of the available downrange capabilities of the various trajectories with given values of corridor depth is shown in figure 28. These data represent the widest variation between maximum and minimum range for combinations of entrance angles corresponding to the given values of corridor depth. Trajectory 1 is seen to give limited range capability because, as stated previously, it skips up to the edge of the atmosphere and is therefore sensitive to range control. Trajectories 2, 3, and 4 with range control only below circular velocity give about 200 miles of range capability for a 35-mile corridor depth and about 1,500 to 2,500 miles for the minimum corridor depths. The use of a two-step range input above circular velocity gives about 1,500 to 3,000 miles of additional range capability.

SUMMARY OF RESULTS

This report has shown that the trajectory motion with lift-drag ratio controlled during entry can be represented as a third-order function with respect to velocity. The first- and second-order feedback terms determine the vehicle's usable corridor depth for entries from supercircular velocity. These terms damp the vehicle's trajectory in such a way that the vehicle does not skip out of the atmosphere or exceed specified acceleration limits. Range input, the third-order term of the control system, must have a high value of feedback gain at velocities less than local circular

velocity to insure that range errors are zero by the end of the trajectory, and the range feedback gain must have a low value at higher velocities to insure a stable response.

The study of an L/D = 0.5 vehicle entering at velocities 40 percent above local circular with a maximum acceleration of 10g indicates that using only constant gain rate-of-climb measurements for controlling L/D results in a usable entry corridor of 30 miles out of the 40 miles available. Using only constant gain acceleration error (about a reference trajectory) inputs gives a maximum usable corridor of about 38 miles, but the actual trajectory oscillates about the reference trajectory. Combining the acceleration and rate-of-climb inputs results in a maximum usable corridor depth of about 37 miles and the vehicle is on the reference trajectory by the time it is near circular velocity.

The attainable downrange increment is about 1,000 miles within a 25-mile corridor depth and 2,000 miles within a 10-mile corridor depth if the constant range input gain is used only at velocities below circular. In addition, if a low value of range input gain is used above circular velocity, the attainable downrange increment is about 3,000 miles within a 25-mile corridor depth and 4,000 miles within a 10-mile corridor depth.

Design reference trajectories that skip up to the edge of the atmosphere in order to extend the range have sensitive control problems and decrease usable corridor depth. Design reference trajectories which stay well within the atmosphere provide larger usable corridor depths.

Ames Research Center
National Aeronautics and Space Administration
Moffett Field, Calif., Aug. 24, 1962

APPENDIX A

LINEARIZED EQUATIONS FOR MOTION ABOUT A REFERENCE TRAJECTORY

An approximate form of the trajectory dynamics about a reference trajectory can be obtained by a linearization of the following Chapman equation from reference 15.

$$Z'' - \frac{Z'}{\bar{u}} + \frac{Z}{\bar{u}^2} - \frac{1 - \bar{u}^2}{\bar{u}^2 Z} = - \frac{\sqrt{\beta r}\ (L/D)}{\bar{u}} \tag{A1}$$

By letting $\Delta Z''$, $\Delta Z'$, and ΔZ denote the changes away from a reference trajectory, we can write equation (A1) in the following manner:

$$(Z''_{ref} + \Delta Z'') - \frac{Z'_{ref} + \Delta Z'}{\bar{u}} + \frac{Z_{ref} + \Delta Z}{\bar{u}^2}$$

$$- \frac{1 - \bar{u}^2}{\bar{u}^2 (Z_{ref} + \Delta Z)} \left(\frac{Z_{ref} - \Delta Z}{Z_{ref} - \Delta Z} \right) = - \frac{\sqrt{\beta r}\ (L/D)}{\bar{u}} \tag{A2}$$

Now linearizing this equation by neglecting ΔZ^2 compared to Z^2_{ref} changes the equation to

$$\Delta Z'' - \frac{\Delta Z'}{\bar{u}} + \left(\frac{1}{\bar{u}^2} + \frac{1 - \bar{u}^2}{\bar{u}^2 Z^2_{ref}} \right) \Delta Z$$

$$= -Z''_{ref} + \frac{Z'_{ref}}{\bar{u}} - \left(\frac{1}{\bar{u}^2} - \frac{1 - \bar{u}^2}{\bar{u}^2 Z^2_{ref}} \right) Z_{ref} - \frac{\sqrt{\beta r}\ (L/D)}{\bar{u}} \tag{A3}$$

This is a linear differential equation in ΔZ with variable coefficients. The left side of the equation contains the "characteristic equation" which determines dynamics of the trajectory about the reference trajectory described on the right The right side of the equation with $L/D = (L/D)_{ref}$ is identical to the Chapman equation for the reference trajectory and can be set equal to zero.

Since $- \sqrt{\beta r}\ \bar{u} Z_{ref} = A_{ref}$ and the influence of $1/\bar{u}^2$ is small during most of the trajectory compared with $(1 - \bar{u}^2)/\bar{u}^2 Z^2$ the equation becomes:

$$\Delta Z'' - \frac{1}{\bar{u}} \Delta Z' + \frac{\beta r(1 - \bar{u}^2)}{A_{ref}^2} \Delta Z = - \frac{\sqrt{\beta r}}{\bar{u}} \Delta \left(\frac{L}{D}\right) \tag{A4}$$

This equation can be written in standard operator notation as follows: (note that $d\bar{u}$ in eq. (A1) is negative during solution of an entry trajectory):

$$\left[s^2 + \frac{1}{\bar{u}} s + \frac{\beta r(1 - \bar{u}^2)}{A_{ref}^2}\right] \Delta Z = \frac{-\sqrt{\beta r}}{\bar{u}} \Delta \left(\frac{L}{D}\right) \tag{A5}$$

The dynamics described by adding various types of control input, $\Delta(L/D)$, will be discussed in the following sections.

CONSTANT L/D

With the L/D held constant during an entry trajectory there is no $\Delta(L/D)$ introduced so that the characteristic equation becomes:

$$s^2 + \frac{1}{\bar{u}} s + \frac{\beta r(1 - \bar{u}^2)}{A_{ref}^2} = 0$$

The frequency and damping at local points along the trajectory from this second-order equation are approximately:

Damping

$$2\zeta\omega_n \approx \frac{1}{\bar{u}}, \text{ radians/unit of } \bar{u}$$

Natural frequency

$$\omega_n^2 \approx \frac{\beta r(1 - \bar{u}^2)}{A_{ref}^2}, \text{ (radians/unit of } \bar{u})^2$$

The important features to be noted here are that the damping ($2\zeta\omega_n$) is small and increases with decreasing velocity, and that spring constant (ω_n^2) is positive, and thus the system is stable, when $\bar{u} < 1$.

Figure 29 presents typical dynamics of a vehicle flown at constant L/D for a subcircular trajectory. As shown in figure 29(a) the vehicle tends to oscillate around an equilibrium glide trajectory. The dynamics of the vehicle away from equilibrium glide trajectory (fig. 29(b)) as calculated by Chapman equation (A1) and as calculated by the linear approximation of equation (A4) are in fairly good agreement. The agreement becomes worse, however, as the trajectory gets farther away from the reference so that ΔZ^2 is no longer small compared with Z_{ref}^2.

A reference equilibrium glide trajectory can be approximated by simplifying the right side of equation (A3) which mathematically describes the reference trajectory. In reference 15 it is noted that, since for equilibrium glide Z''_{ref} and Z'_{ref} are essentially zero and Z_{ref} is much smaller than $(1 - \bar{u}^2)/Z_{ref}$, the right side of the equation reduces to the well-known approximation for equilibrium glide:

$$-A_{ref} \approx \frac{1 - \bar{u}^2}{(L/D)_{ref}}$$

For the particular case of an equilibrium glide reference trajectory this value of A_{ref} can be substituted into the characteristic equation so that:

Damping

$$2\zeta\omega_n \approx \frac{1}{\bar{u}}, \text{ radians/unit of } \bar{u}$$

Natural frequency

$$\omega_n^2 \approx \frac{\beta r(L/D)^2}{1 - \bar{u}^2}, \text{ (radians/unit of } \bar{u})^2$$

This shows the interesting fact that during a constant L/D entry, the damping $(2\zeta\omega_n)$ of these long-term motions is independent of L/D but the natural frequency of oscillation with respect to velocity is directly proportional to L/D.

RATE-OF-CLIMB CONTROL

The Z function method (ref. 15) expresses rate of climb as: $\dot{h} = \sqrt{g/\beta}\ (\bar{u}Z' - Z)$, fps. The use of rate-of-climb errors with respect to the reference trajectory in controlling L/D is considered in the following manner:

$$\Delta(L/D) = K_1\Delta\dot{h} = K_1\sqrt{g/\beta}\ (\bar{u}\ \Delta Z' - \Delta Z)$$

The $\Delta(L/D)$ can be substituted into equation (A4) so that

$$s^2 + \left(\frac{1}{\bar{u}} - K_1\sqrt{gr}\right)s + \frac{\beta r(1 - \bar{u}^2)}{A_{ref}^2} - \frac{K_1\sqrt{gr}}{\bar{u}} = 0$$

and at each local point along the trajectory, the damping and natural frequency can be approximated by:

Damping

$$2\zeta\omega_n \approx \frac{1}{\bar{u}} - K_1\sqrt{gr}, \text{ radians/unit of } \bar{u}$$

Natural frequency

$$\omega_n^2 \approx \frac{\beta r(1 - \bar{u}^2)}{A_{ref}^2} - \frac{K_1\sqrt{gr}}{\bar{u}}, \text{ (radians/unit of } \bar{u})^2$$

From this approximate solution the important feature of control by rate-of-climb errors can be noted; the gain K_1 must be negative in order to damp the trajectory motion. In turn, this will increase the natural frequency. This increase in ω_n^2 is very slight, however, for gains on the order of those to give near critical damping ($\zeta \approx 1$) so that rate of climb is essentially a first-order feedback quantity, affecting the damping only.

ACCELERATION CONTROL

The Z function method (ref. 15) expresses acceleration as $A = -\sqrt{\beta r}\,\bar{u}Z$, g units. The use of acceleration errors with respect to the reference trajectory in controlling L/D is considered in the following manner:

$$\Delta(L/D) = K_2\Delta A = -K_2\sqrt{\beta r}\,\bar{u}\,\Delta Z$$

The $\Delta(L/D)$ can be substituted into equation (A4) so that,

$$s^2 + \frac{1}{\bar{u}}s + \beta r\left(\frac{1 - \bar{u}^2}{A_{ref}^2} - K_2\right) = 0$$

and at each local point along the trajectory the damping and frequency can be approximated by:

Damping

$$2\zeta\omega_n \approx \frac{1}{\bar{u}}, \text{ radians/unit of } \bar{u}$$

Frequency

$$\omega_n^2 \approx \beta r\left(\frac{1 - \bar{u}^2}{A_{ref}^2} - K_2\right), \text{ (radians/unit of } \bar{u})^2$$

From this approximate solution the important features of control by acceleration errors can be noted: a negative value of gain K_2 will increase the natural frequency (ω_n^2) and will not affect the damping ($2\zeta\omega_n$) along the trajectory.

RANGE CONTROL

The Z function method (ref. 15) expresses range as:

$$R = \frac{r}{5280\sqrt{\beta r}} \int_{\bar{u}_2}^{\bar{u}_1} \frac{1}{Z}\, d\bar{u}$$

The use of range errors with respect to the reference trajectory in controlling L/D is considered in the following manner:

$$\Delta(L/D) = K_3\Delta R = K_3 \frac{r}{5280\sqrt{\beta r}} \left[\int_{\bar{u}_2}^{\bar{u}_1} \frac{(Z_{ref} - \Delta Z)d\bar{u}}{(Z_{ref} - \Delta Z)(Z_{ref} + \Delta Z)} - \int_{\bar{u}_2}^{\bar{u}_1} \frac{d\bar{u}}{Z_{ref}} \right]$$

Neglecting ΔZ^2 compared to Z_{ref}^2 this becomes

$$\Delta(L/D) = K_3 \frac{r}{5280\sqrt{\beta r}} \int_{\bar{u}_2}^{\bar{u}_1} \frac{\Delta Z}{Z_{ref}^2}\, d\bar{u}$$

The $\Delta(L/D)$ can be substituted into equation (A4) and the motion at local points along the trajectory (i.e., $Z'_{ref}\, du \ll Z_{ref}$) can be approximated by the following third-order equation:

$$s^3 + \frac{1}{\bar{u}} s^2 + \frac{\beta r(1 - \bar{u}^2)}{A_{ref}^2} s + K_3 \frac{\beta r^2 \bar{u}}{5280\, A_{ref}^2} = 0$$

From this approximate solution, the important features of control by range errors can be noted: The range-input term results in a third-order control system. As with any third-order control system, the gain can be made large enough to cause the system to become unstable. The stability criterion (i.e., Routh's method) is that the system will be unstable when:

$$K_3 > \frac{1 - \bar{u}^2}{\bar{u}^2} \left(\frac{5280}{r} \right)$$

As shown in the text, feedbacks other than range control alone (i.e., acceleration and rate of climb) will add more inner loop damping to the system and allow a larger range gain than the one described here for range input alone.

REFERENCES

1. Eggleston, John M., and Young, John W.: Trajectory Control for Vehicles Entering the Earth's Atmosphere at Small Flight-Path Angles. NASA TR R-89, 1961 (Supersedes NASA MEMO 1-19-59L, 1959.)

2. Wingrove, Rodney C., and Coate, Robert E.: Piloted Simulator Tests of Guidance System Which Can Continuously Predict Landing Point of a Low L/D Vehicle During Atmosphere Reentry. NASA TN D-787, 1961.

3. Foudriat, Edwin C.: Study of the Use of a Terminal Controller Technique for Reentry Guidance of a Capsule-Type Vehicle. NASA TN D-828, 1961.

4. Young, John W.: A Method for Longitudinal and Lateral Range Control for a High Drag Low-Lift Vehicle Entering the Atmosphere of a Rotating Earth. NASA TN D-954, 1961.

5. Dow, Paul C., Fields, Donald P., and Scammell, Frank H.: Automatic Reentry Guidance at Escape Velocity. ARS Preprint 1946-61.

6. Bryson, Arthur E., and Denham, Walter F.: A Guidance Scheme for Supercircular Reentry of a Lifting Vehicle. ARS Preprint 2299-61.

7. Foudriat, Edwin C., and Wingrove, Rodney C.: Guidance and Control During Direct-Descent Parabolic Reentry. NASA TN D-979, 1961.

8. Morth, Raymond, and Speyer, Jason: Control System for Supercircular Entry Maneuvers. IAS Paper 62-3, Jan. 1962.

9. Young, John W., and Goode, Maxwell W.: Fixed-Base Simulator Studies of the Ability of the Human Pilot to Provide Energy Management Along Abort and Deep-Space Entry Trajectories. Proc. of National Aerospace Electronics Conference, Dayton, Ohio, May 14-16, 1962.

10. Chapman, Philip W., and Moonan, Peter J.: Analysis and Evaluation of a Proposed Method for Inertial Reentry Guidance of a Deep Space Vehicle. Proc. National Aerospace Electronics Conference, Dayton, Ohio, May 14-16, 1962.

11. Bryant, J. P., and Frank, M. P.; Supercircular Reentry Guidance for a Fixed L/D Vehicle Employing a Skip for Extreme Ranges. ARS Preprint 2489-62, 1962.

12. Wingrove, Rodney C., and Coate, Robert E.: Lift-Control During Atmosphere Entry From Supercircular Velocity. Proceedings of the IAS National Meeting on Manned Space Flight, St. Louis, Missouri, April 30-May 2, 1962.

13. Chapman, Dean R.: An Analysis of the Corridor and Guidance Requirements for Supercircular Entry Into Planetary Atmospheres. NASA TR R-55, 1960.

14. Wong, Thomas J., and Slye, Robert E.: The Effect of Lift on Entry Corridor Depth and Guidance Requirements for the Return Lunar Flight. NASA TR R-80, 1961.

15. Chapman, Dean R.: An Approximate Analytical Method for Studying Entry Into Planetary Atmospheres. NASA TR R-11, 1959.

16. Slye, Robert E.: An Analytical Method for Studying the Lateral Motion of Atmosphere Entry Vehicles. NASA TN D-325, 1960.

17. Creer, Brent Y., Smedal, Harald A., Capt. USN (MC), and Wingrove, Rodney C.: Centrifuge Study of Pilot Tolerance to Acceleration and the Effects of Acceleration on Pilot Performance. NASA TN D-337, 1960.

18. Becker, J. V., Baradell, D. L., and Pritchard, E. B.: Aerodynamics of Trajectory Control for Reentry at Escape Speed. Astronautica Acta., vol. 7, 1961.

19. Sommer, Simon C., and Short, Barbara J.: Point Return From a Lunar Mission for a Vehicle That Maneuvers Within the Earth's Atmosphere. NASA TN D-1142, 1961.

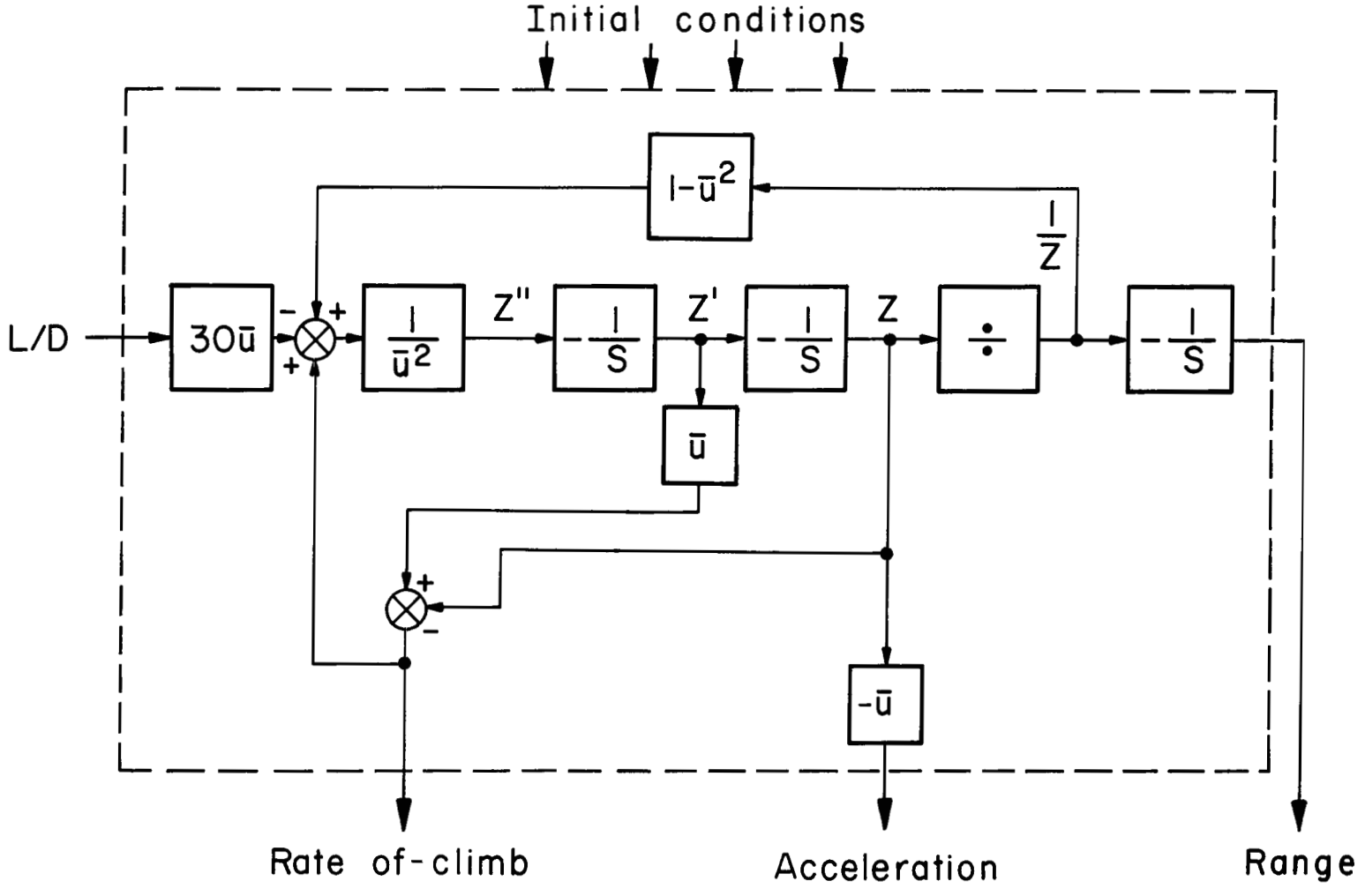

Figure 1.- Block diagram of simulated entry equation.

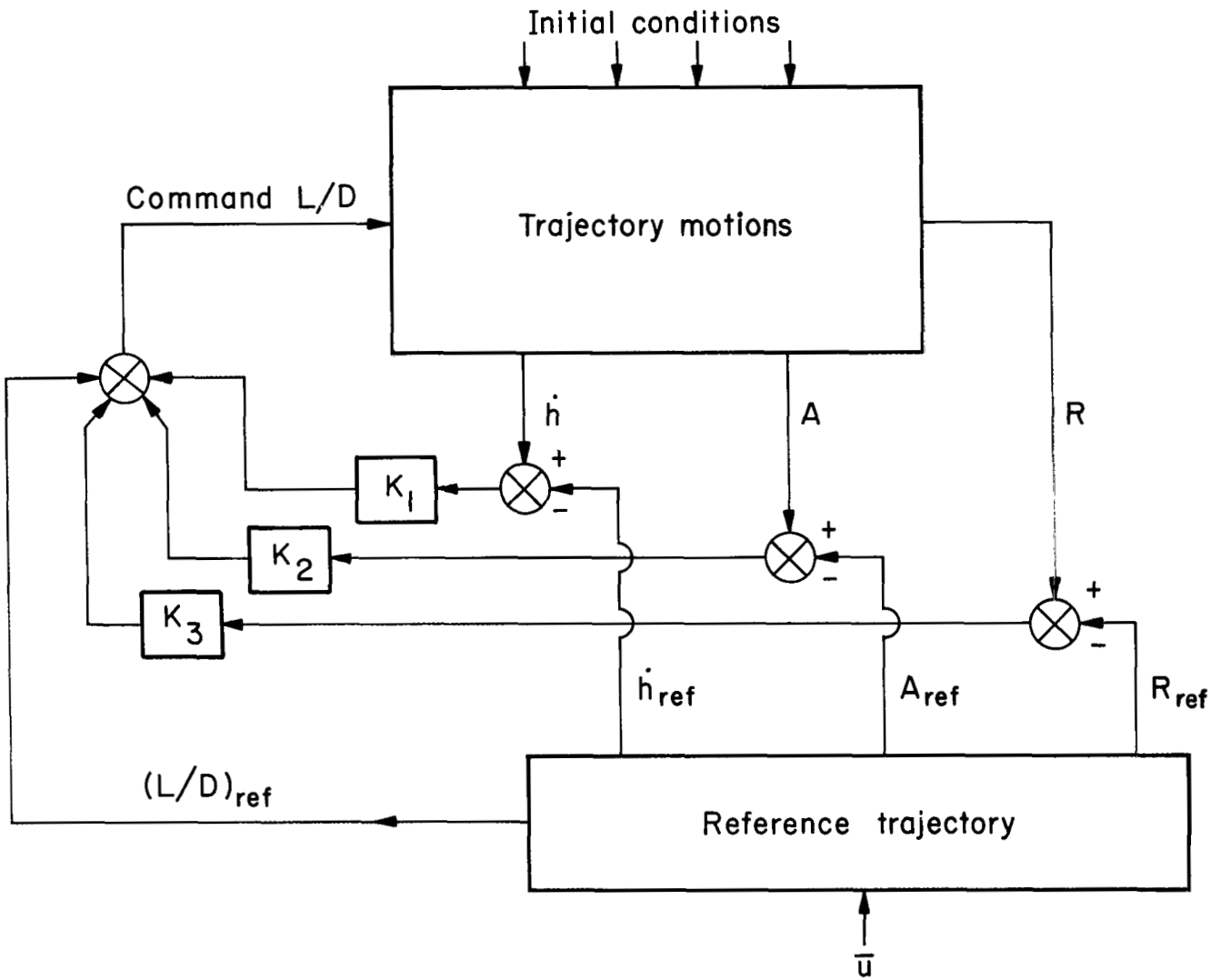

Figure 2.- Block diagram of simulated control system.

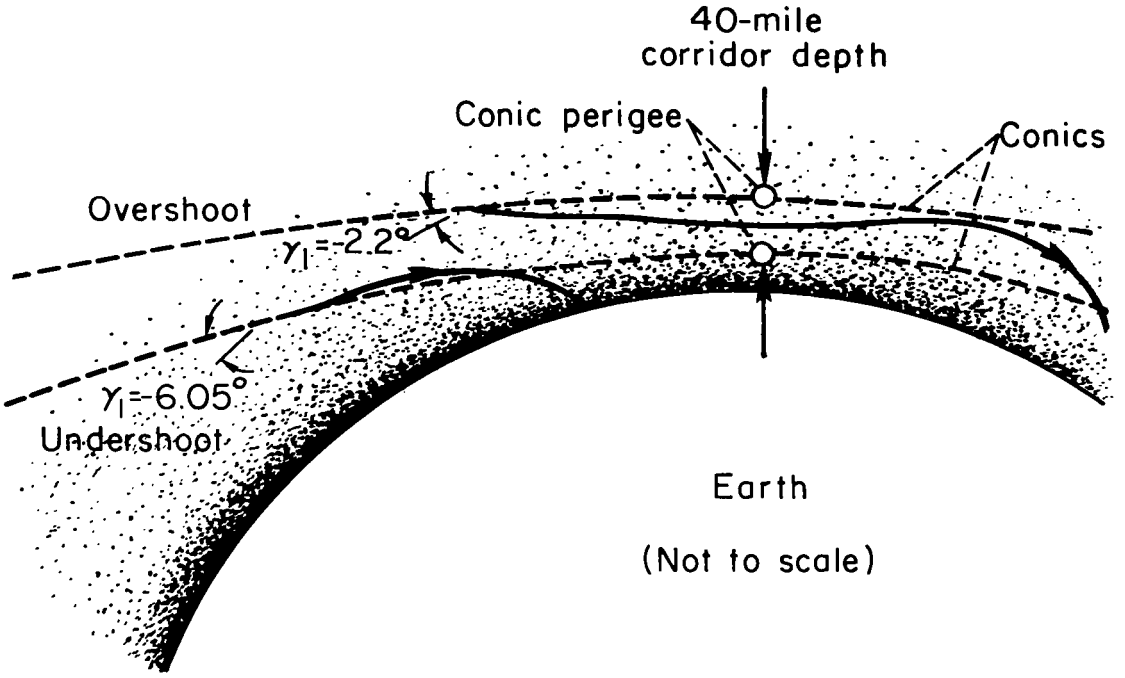

Figure 3.- Definition of corridor depth.

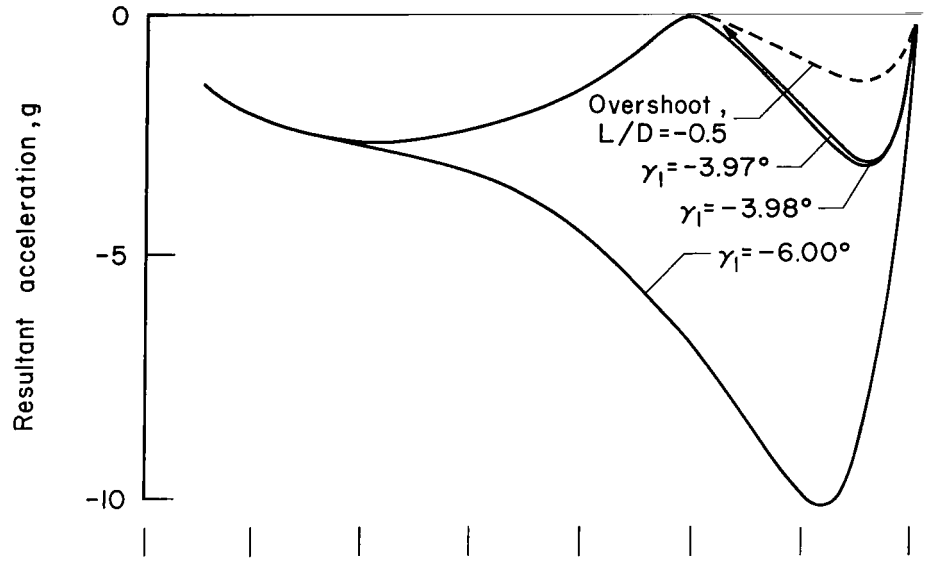

(a) Acceleration

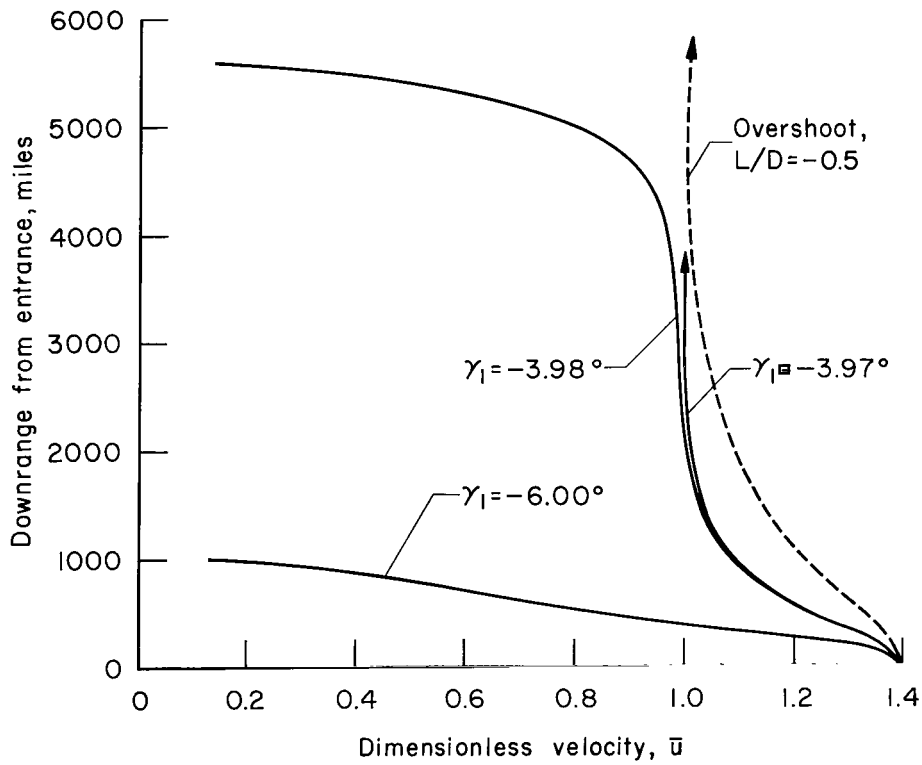

(b) Downrange

Figure 4.- Entry trajectories controlled as a function of rate of climb with K_1 = -0.001/fps.

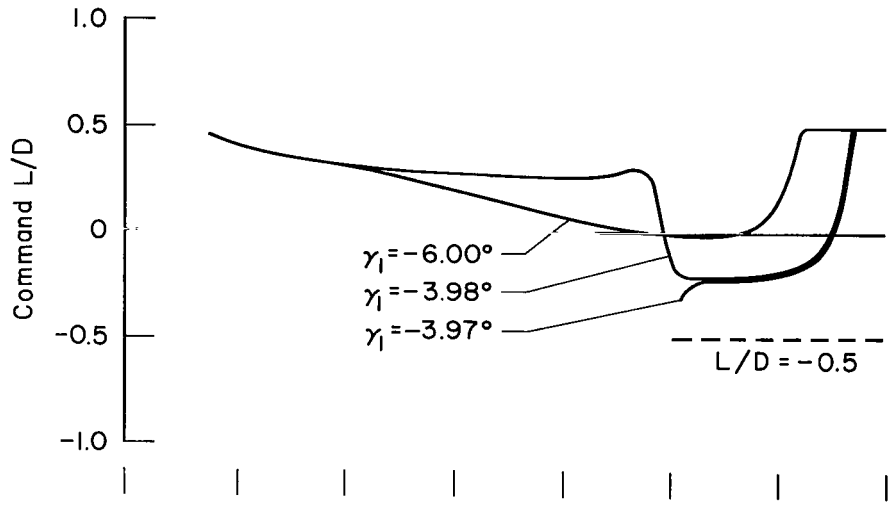

(c) Command L/D.

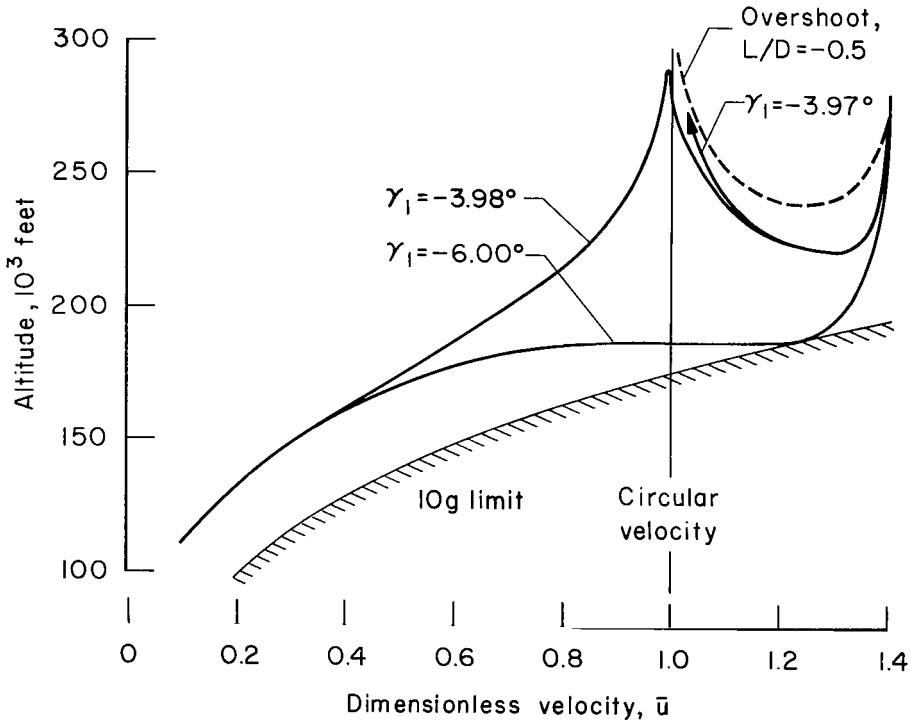

(d) Altitude, W/C_DS = 48 psf.

Figure 4.- Concluded.

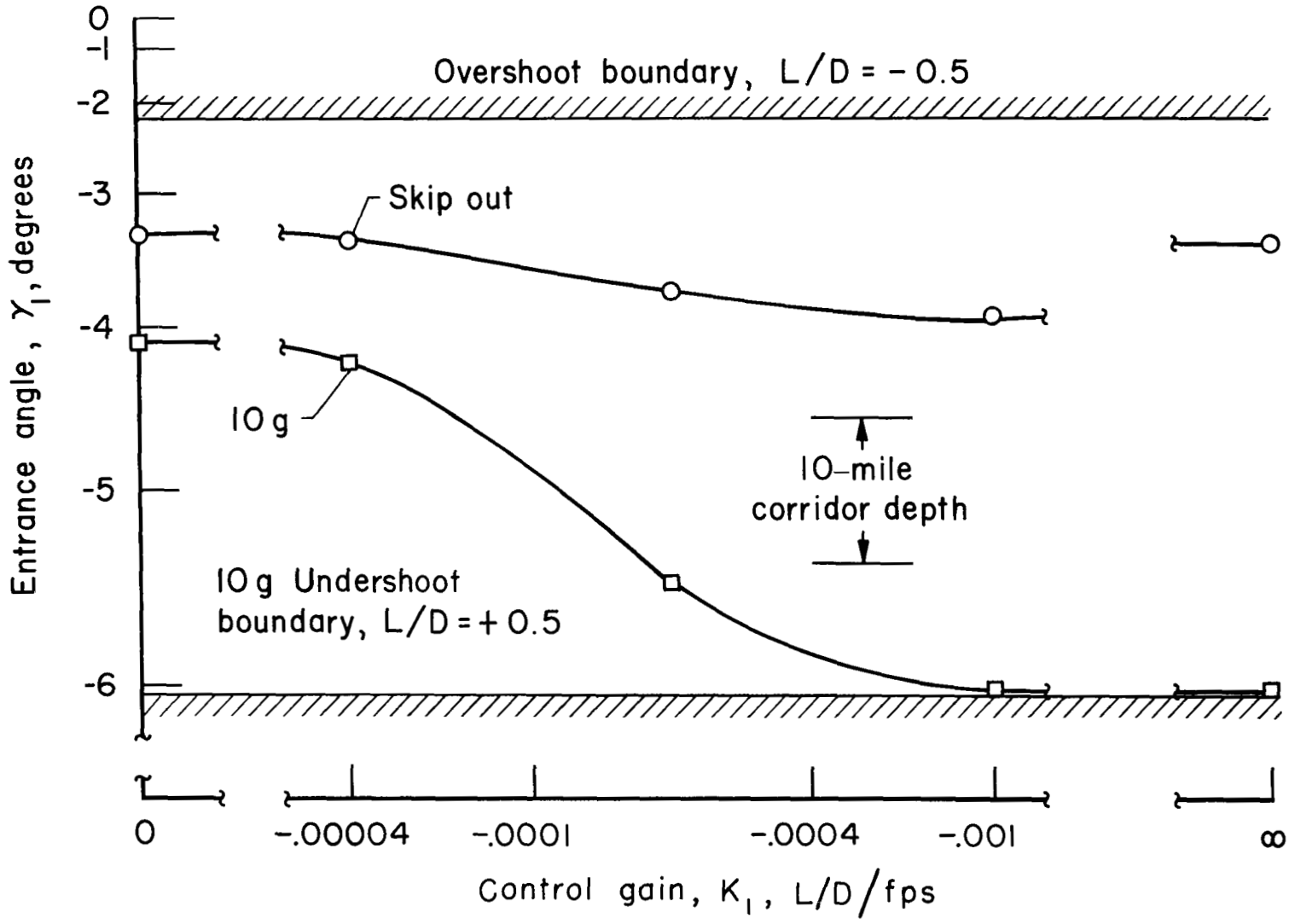

Figure 5.- Effect of control gain, K_1, on usable corridor depth.

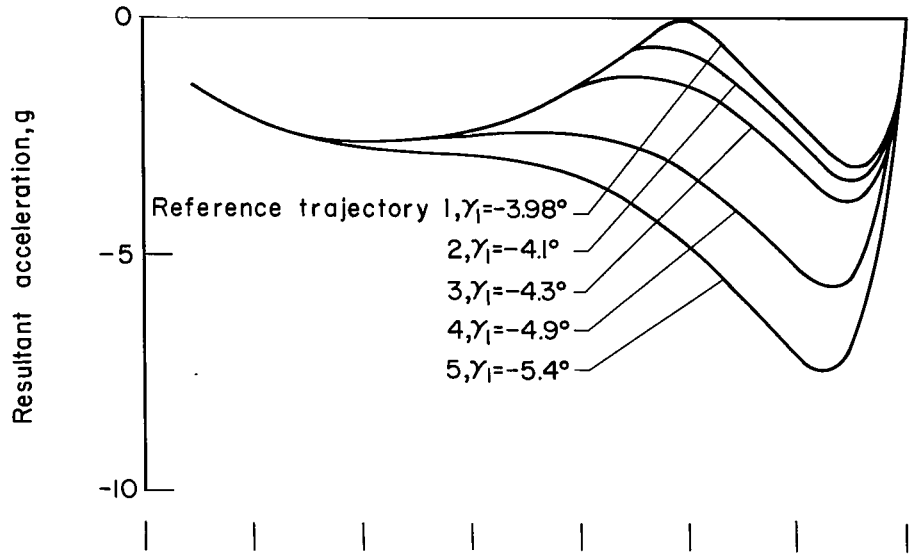

(a) Acceleration

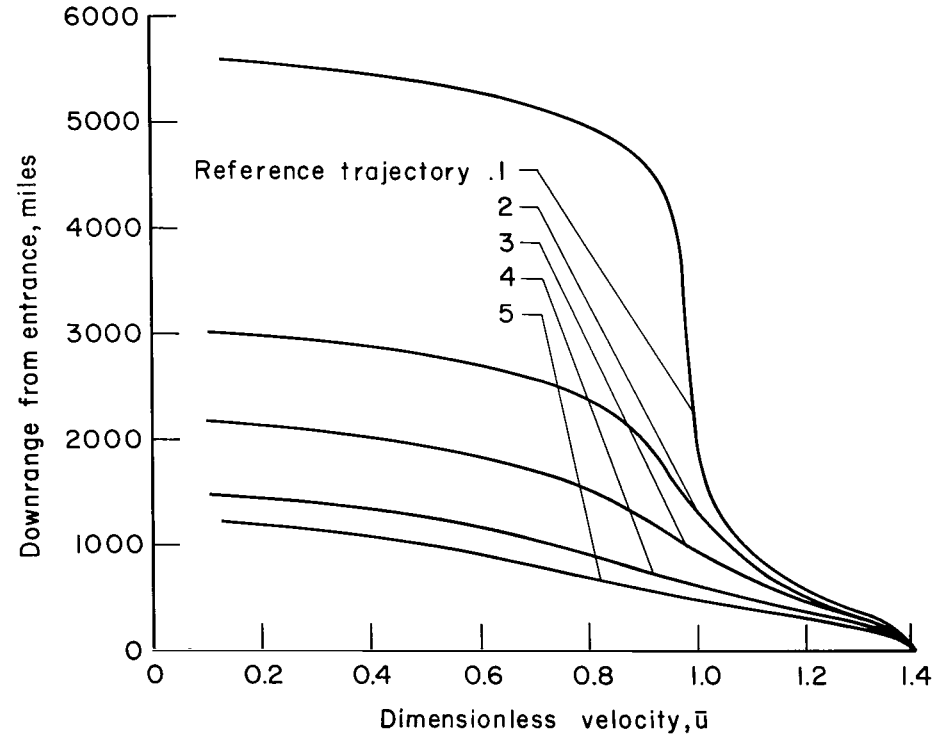

(b) Downrange

Figure 6.- Family of reference trajectories based on rate of climb control with K_1 = -0.001/fps.

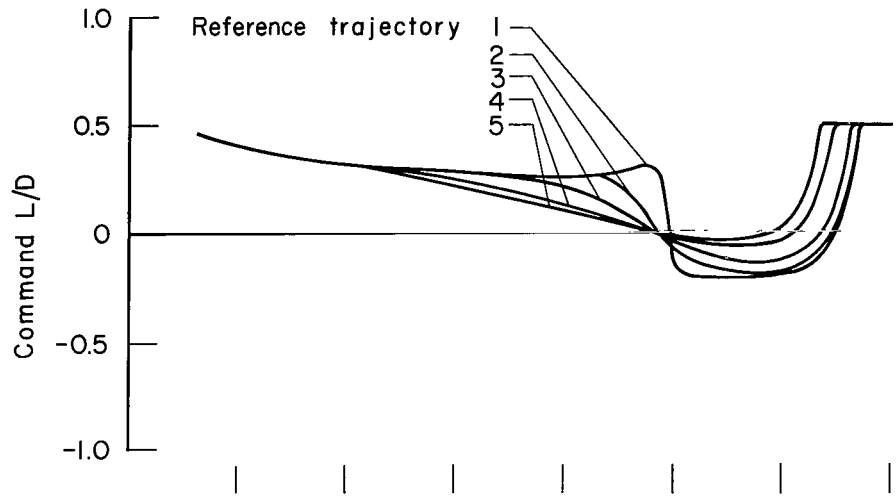

(c) Command L/D.

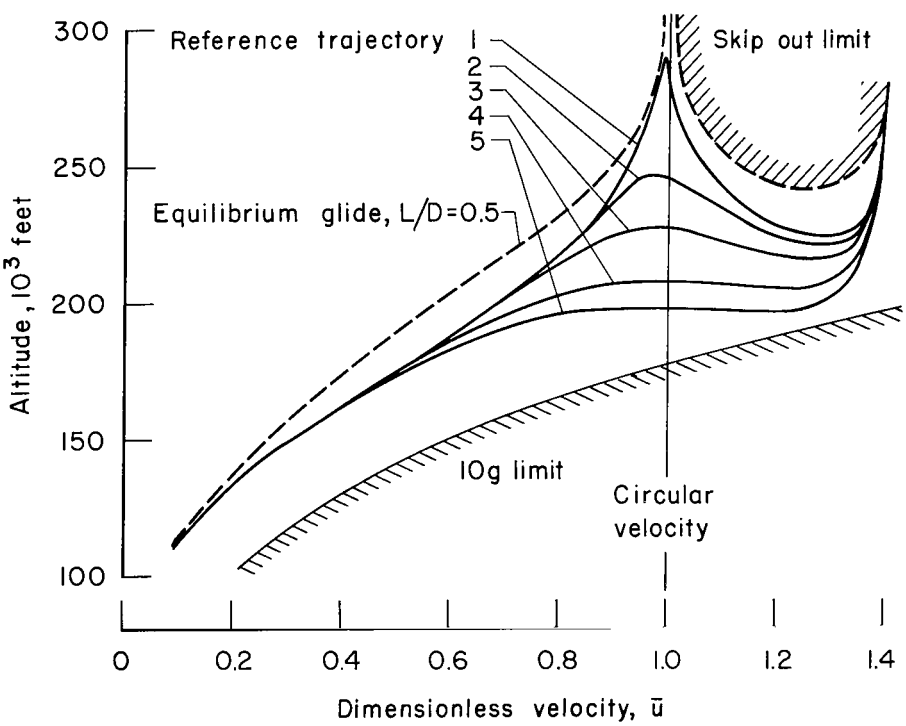

(d) Altitude, W/C_DS = 48 psf.

Figure 6.- Concluded.

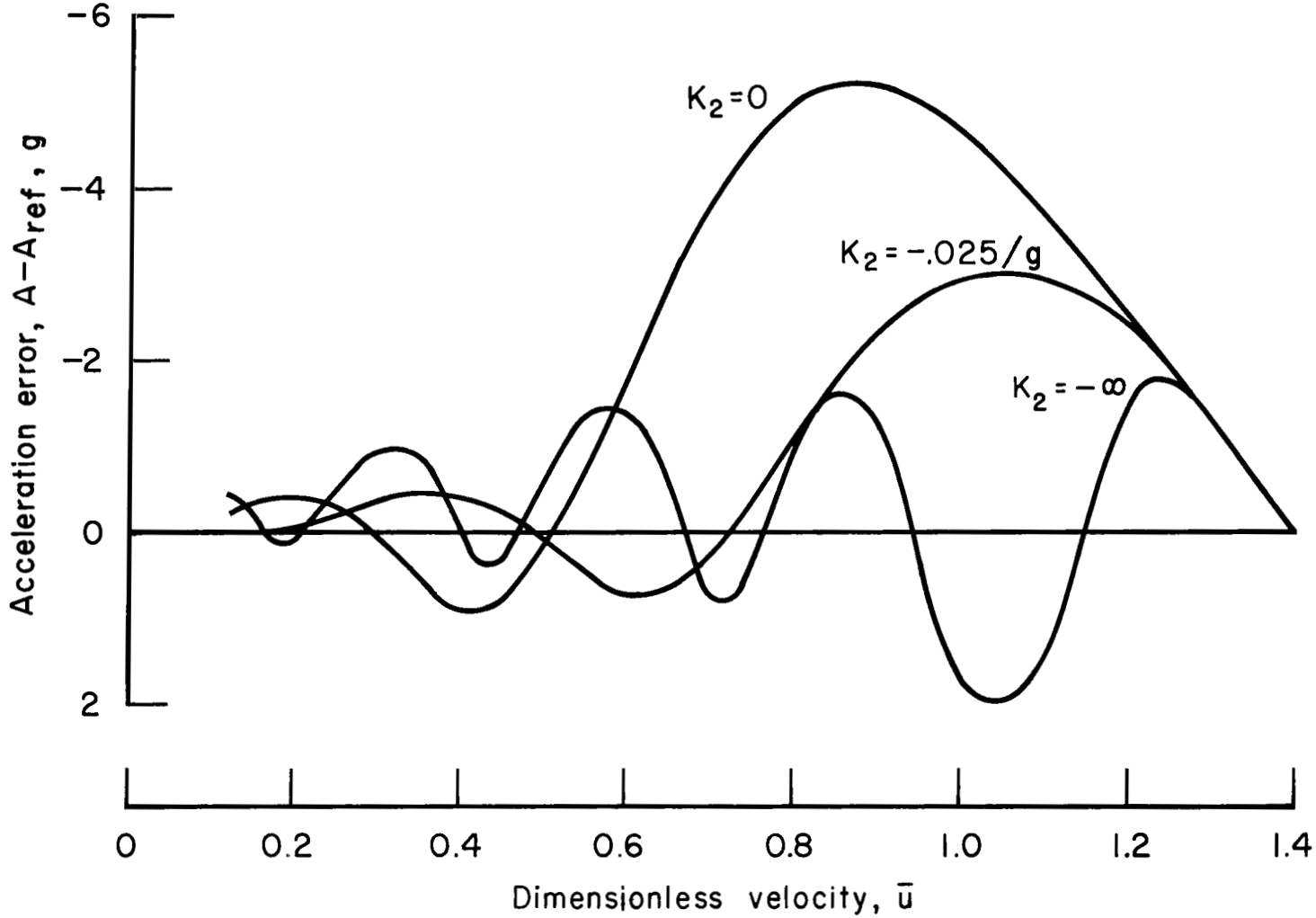

Figure 7.- Effect of control gain, K_2, on acceleration error for acceleration control with reference trajectory 4; $\gamma_1 = -5.5^\circ$.

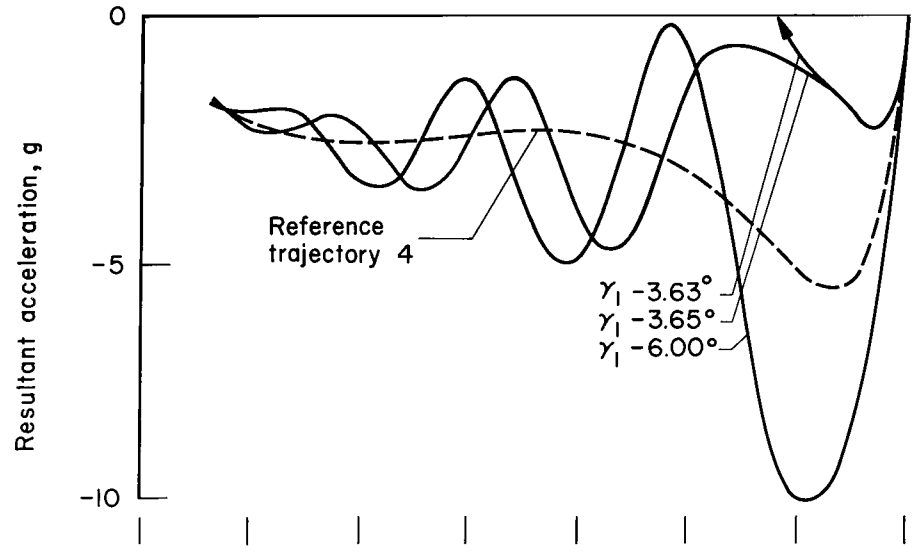

(a) Acceleration

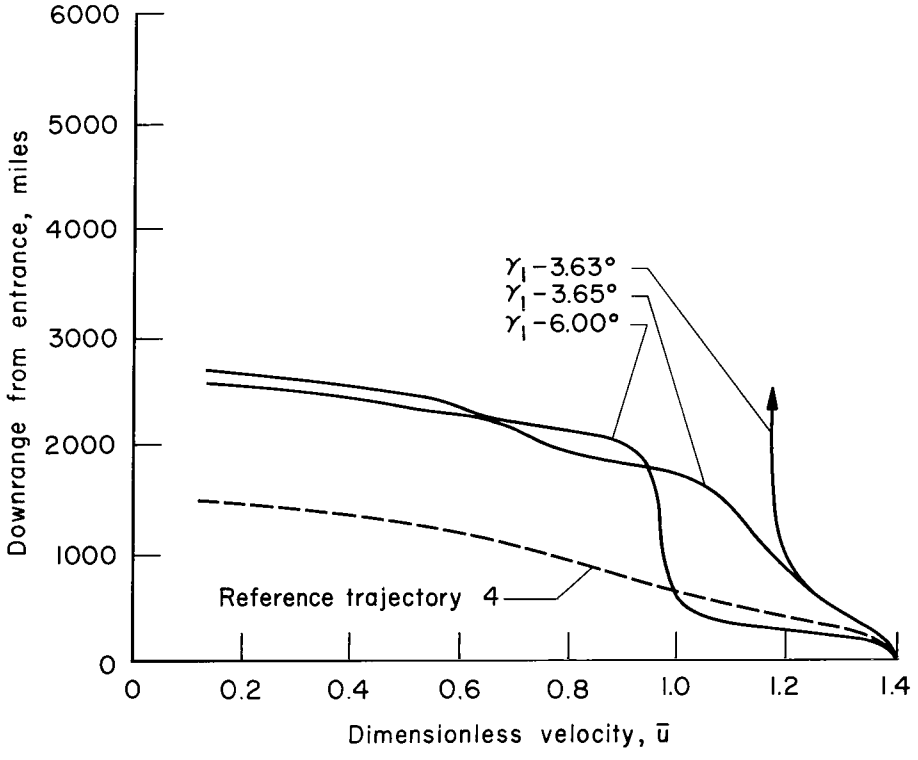

(b) Downrange

Figure 8.- Control to reference trajectory 4 using acceleration control with $K_2 = -0.33/g$.

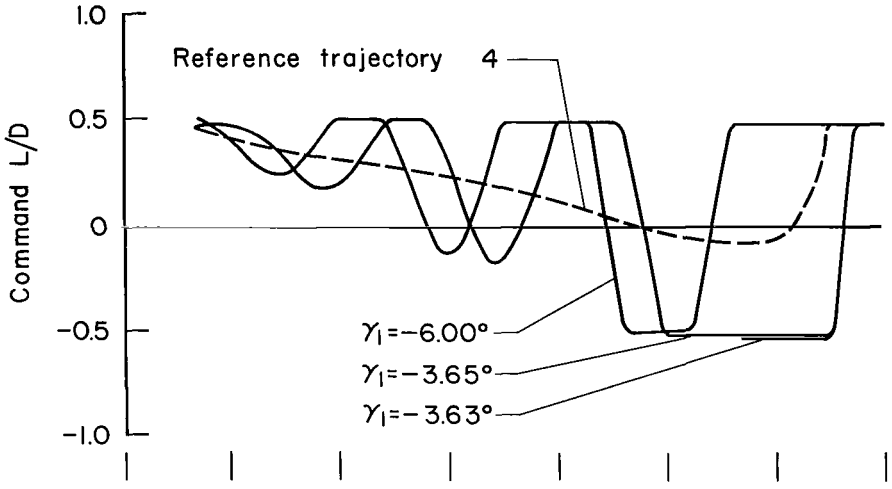

(c) Command L/D.

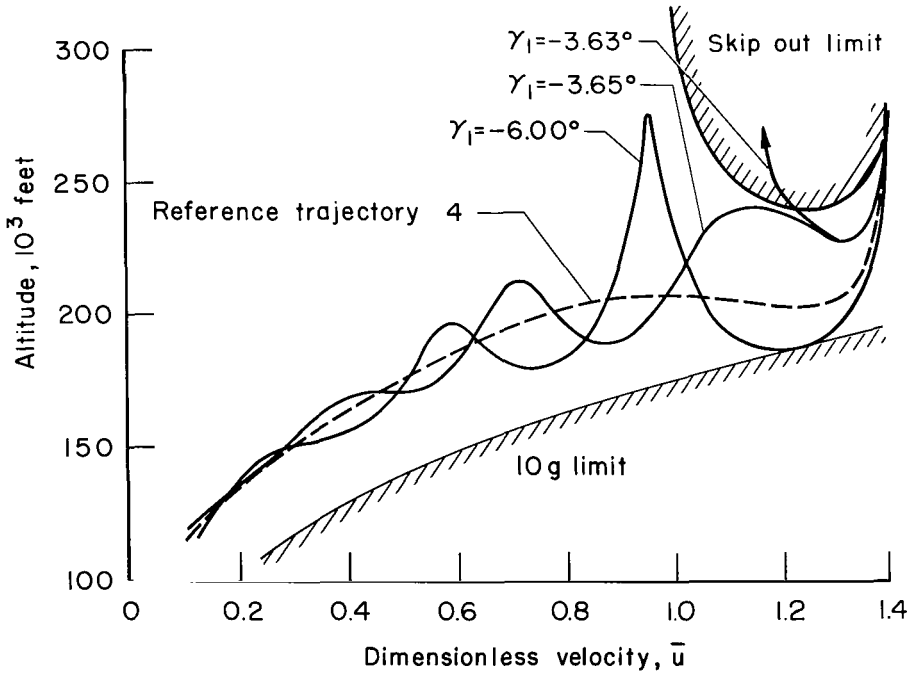

(d) Altitude, W/C_DS = 48 psf.

Figure 8.- Concluded.

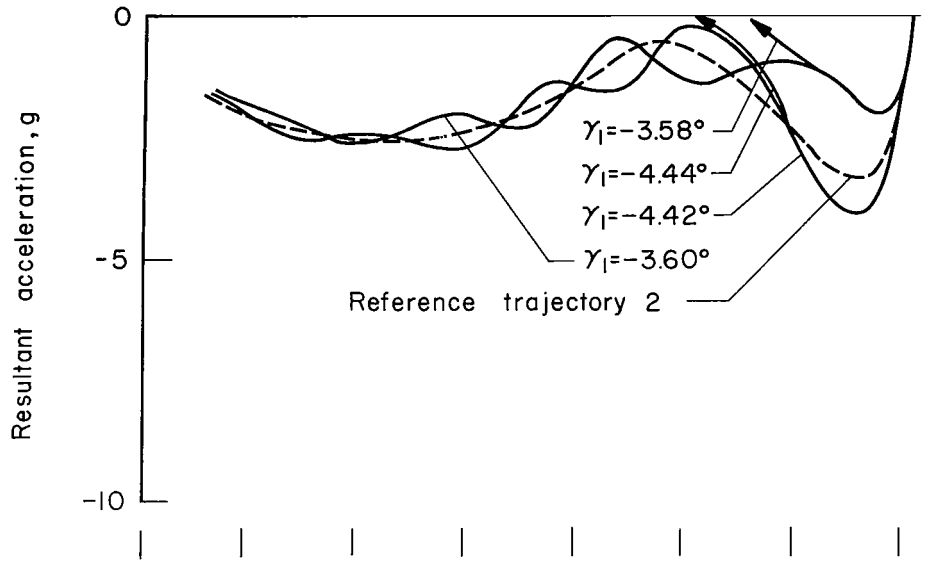

(a) Acceleration

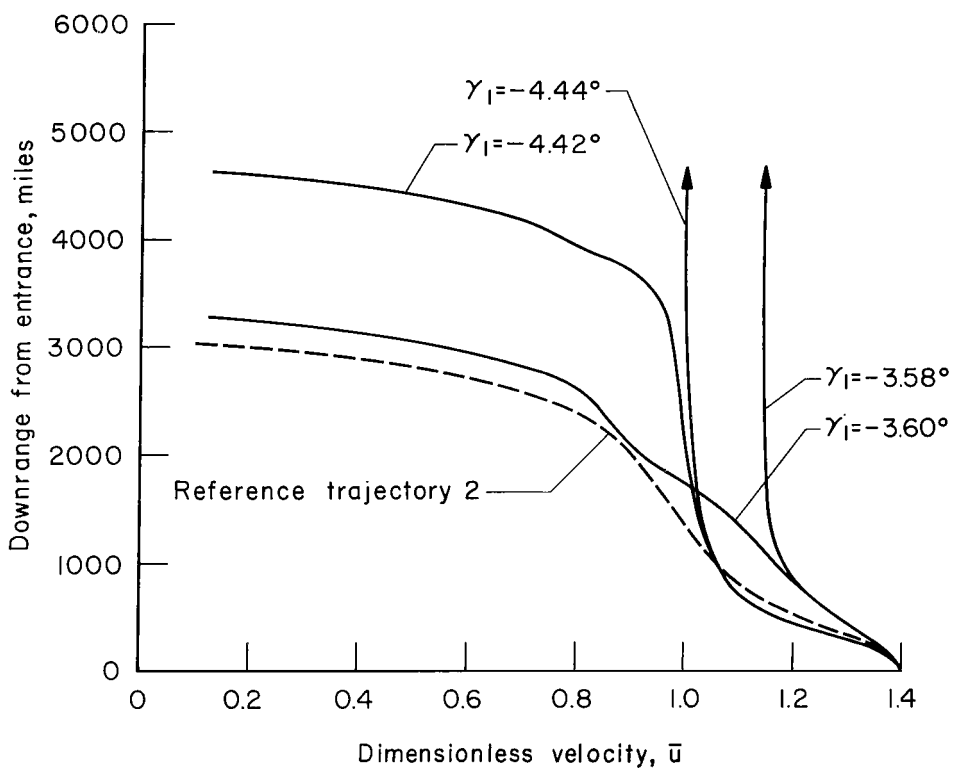

(b) Downrange

Figure 9.- Control to reference trajectory 2 using acceleration control with $K_2 = -0.33/g$.

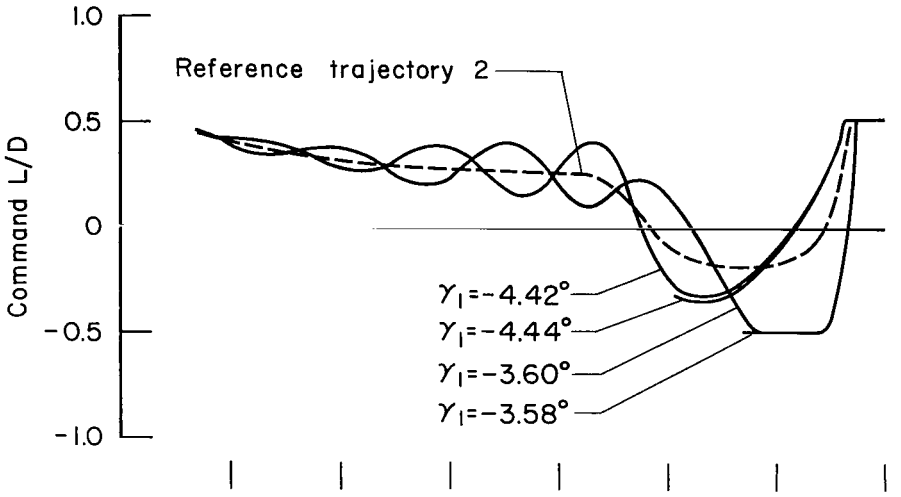

(c) Command L/D.

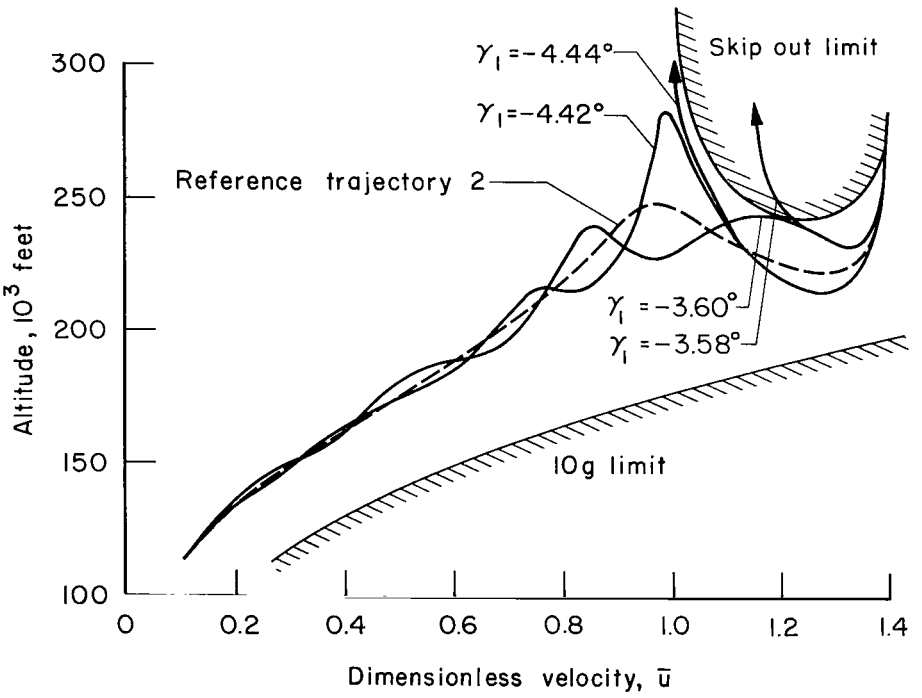

(d) Altitude, W/C_DS = 48 psf.

Figure 9.- Concluded.

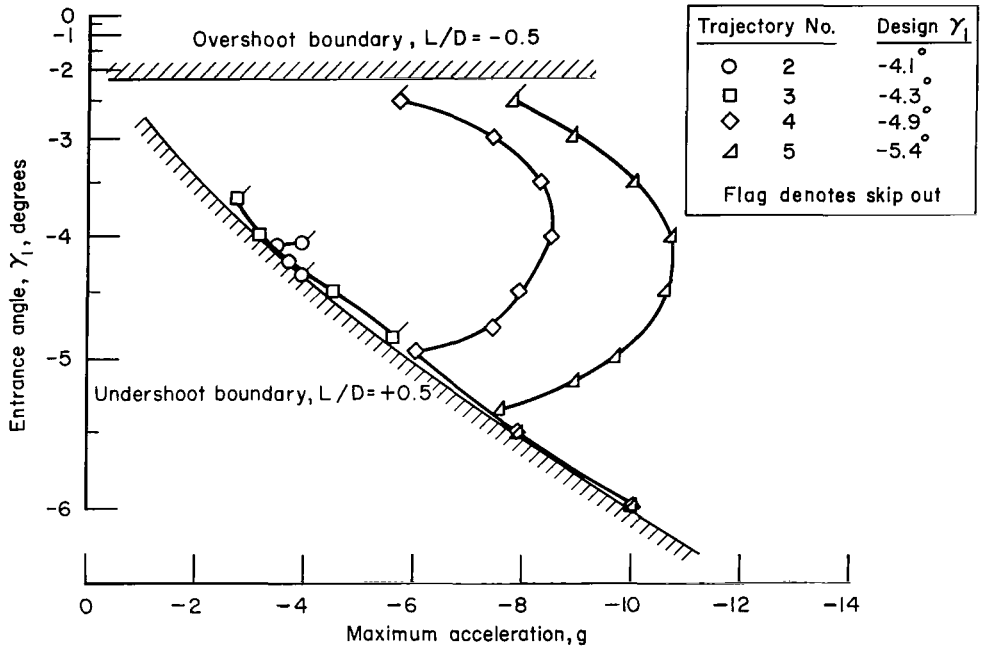

(a) $K_2 = -\infty$

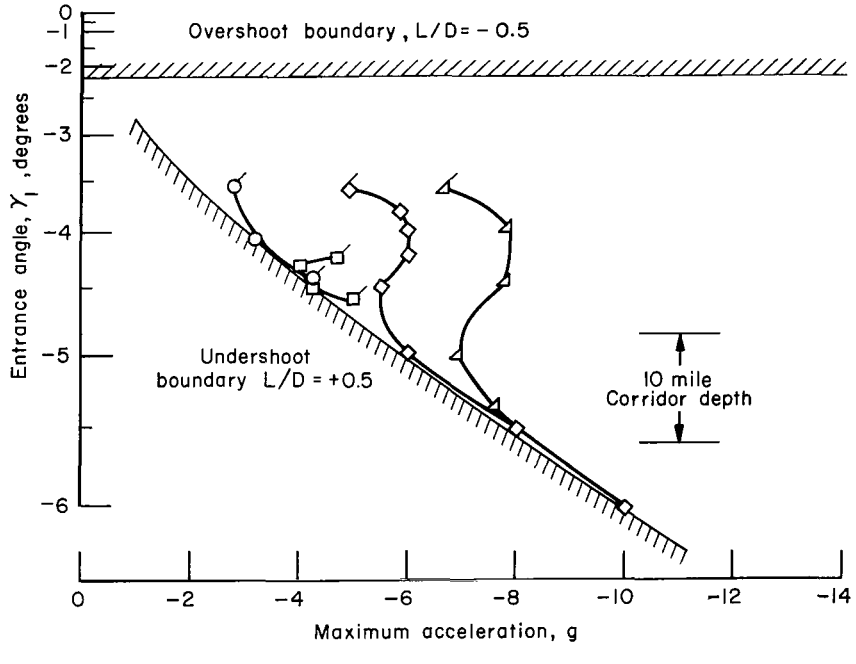

(b) $K_2 = -0.33/g$

Figure 10.- Maximum peak acceleration as a function of entrance angle for acceleration control.

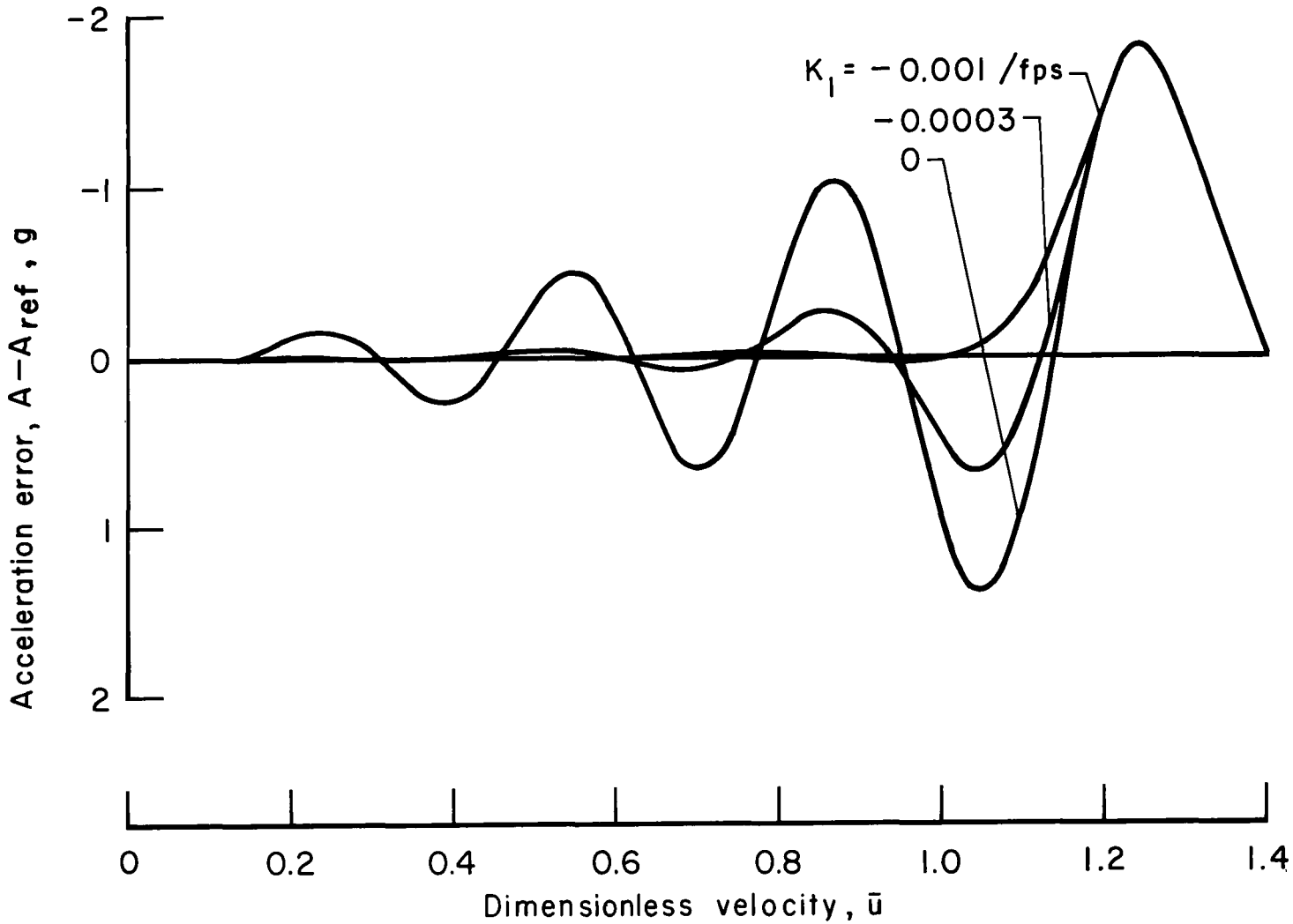

Figure 11.- Effect of control gain, K_1, on acceleration error for combined acceleration and rate of climb control with reference trajectory 4; $\gamma_1 = -5.5^\circ$, $K_2 = -0.33/g$.

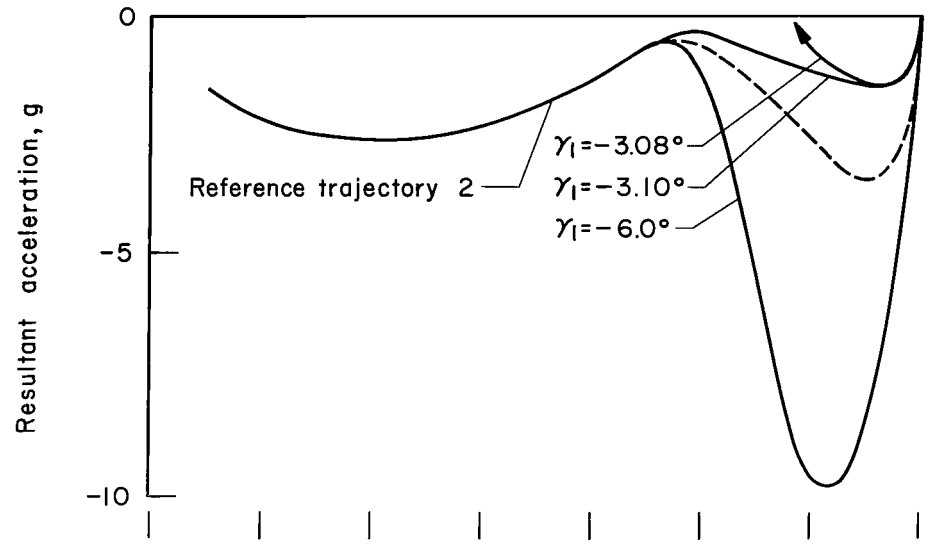

(a) Acceleration

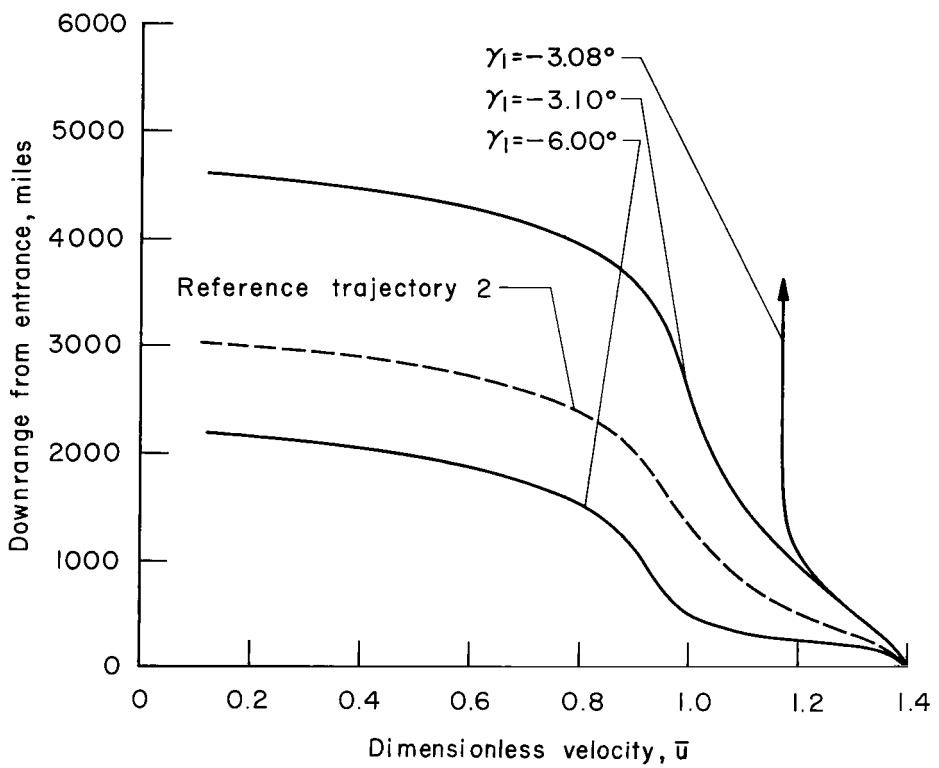

(b) Downrange

Figure 12.- Control to reference trajectory 2 for combined acceleration and rate of climb control with K_1 = -0.001/fps and K_2 = -0.33/g.

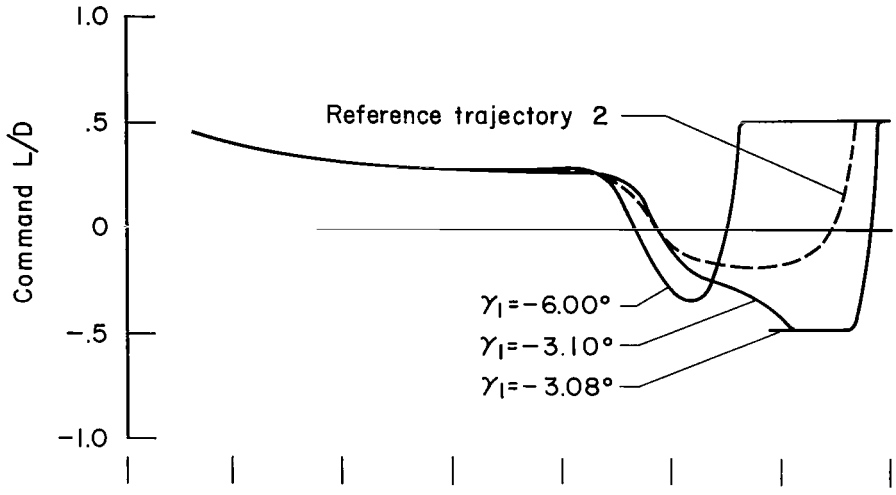

(c) Command L/D.

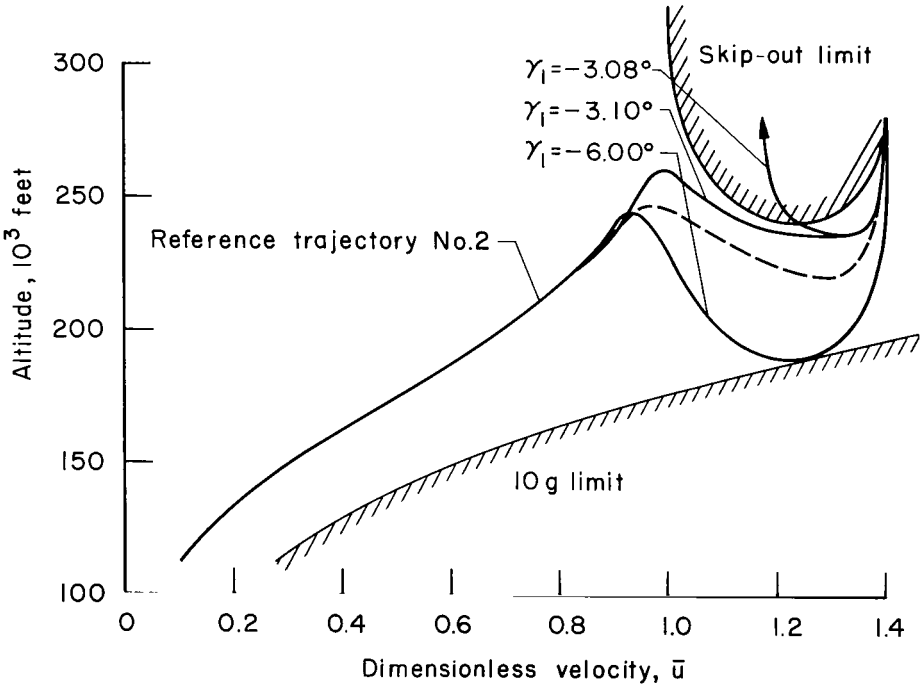

(d) Altitude, W/C_DS = 48 psf.

Figure 12.- Concluded.

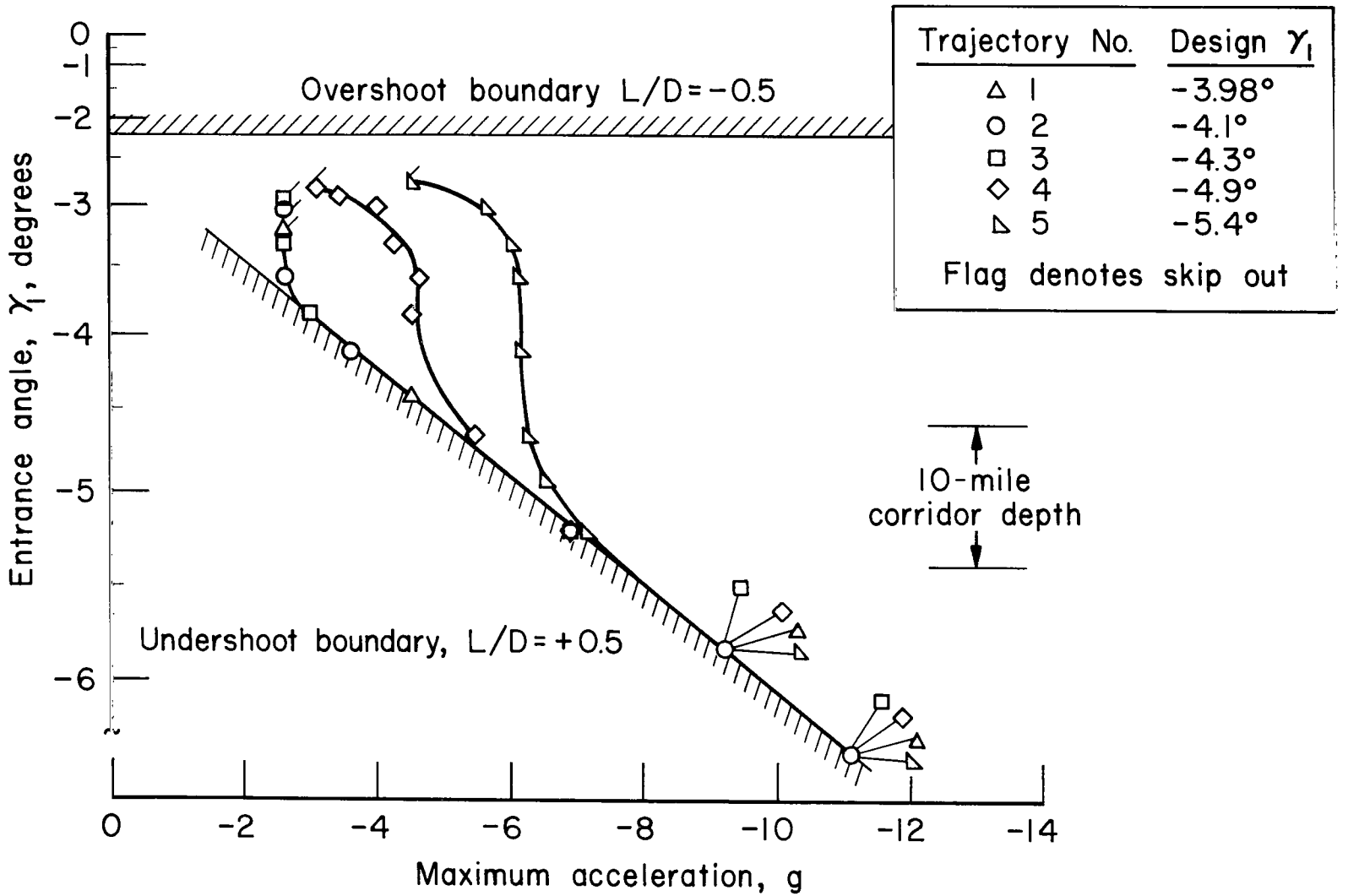

Figure 13.- Maximum peak acceleration as a function of entrance angle for combined acceleration and rate of climb control with K_1 = -0.001/fps and K_2 = -0.33/g.

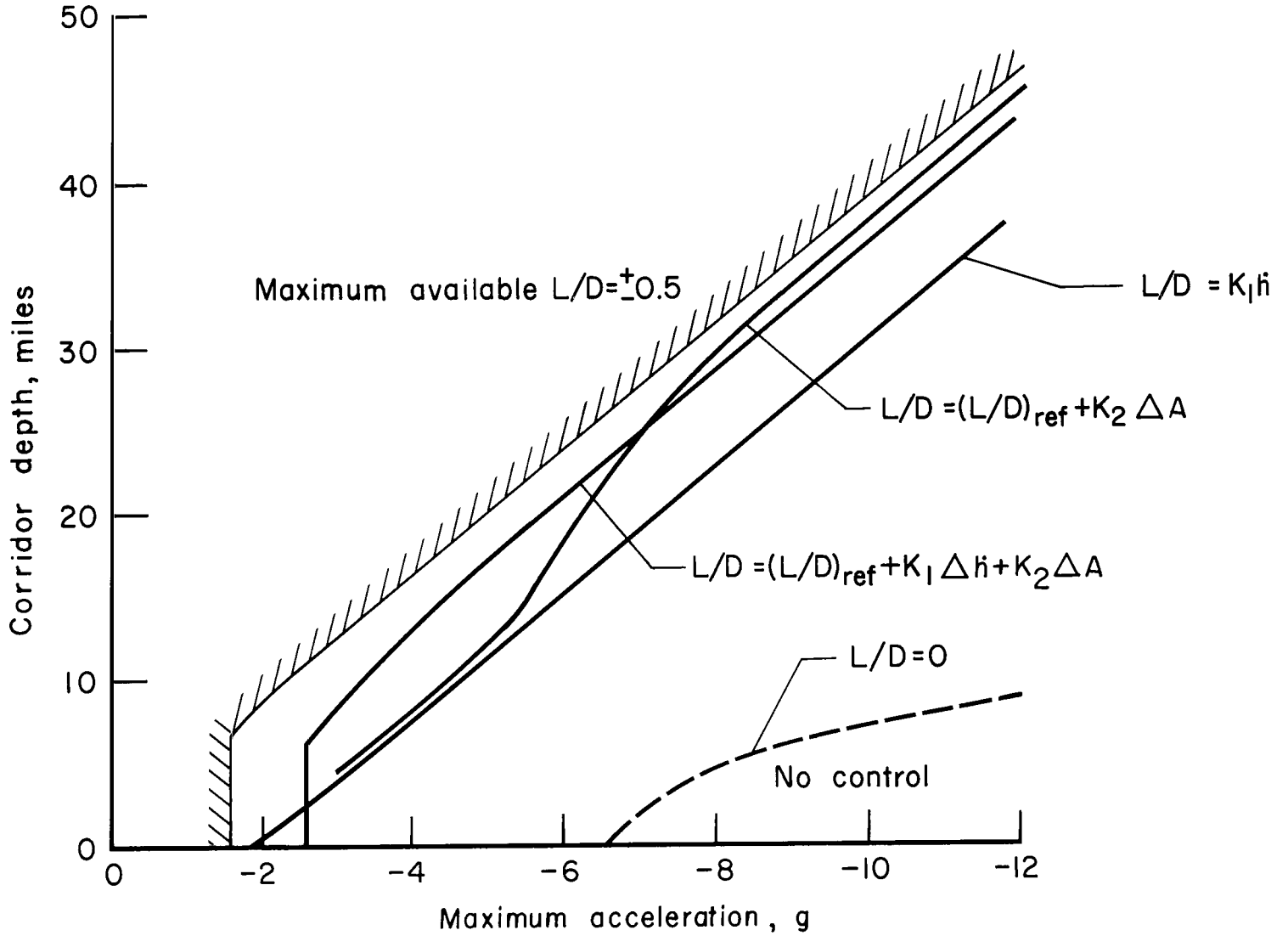

Figure 14.- Usable corridor depth for various methods of trajectory control.

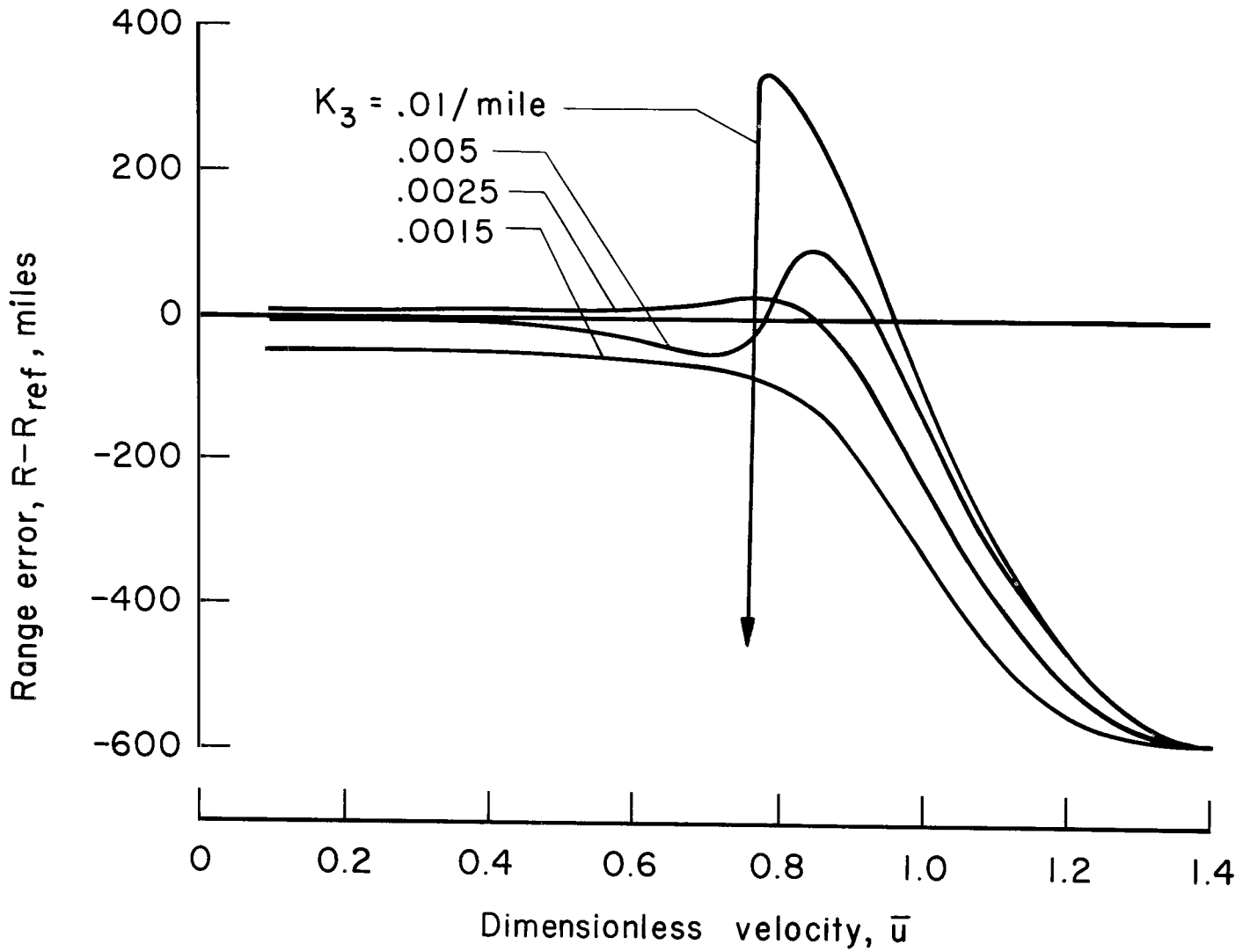

Figure 15.- Effect of control gain, K_3, on range error using range control for trajectory 3 with $K_1 = -0.001/\text{fps}$ and $K_2 = -0.33/g$; $\gamma_1 = -4.3^\circ$.

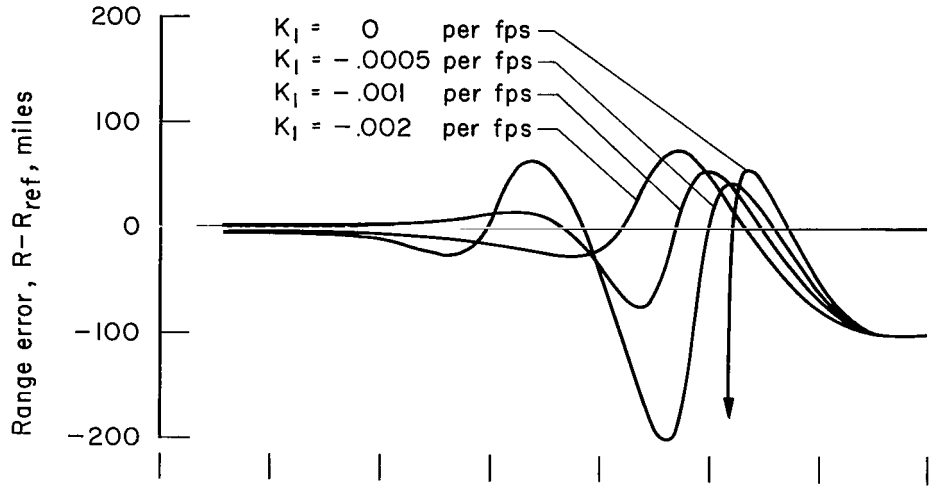

(a) Effect of K_1 with $K_2 = -0.33/g$.

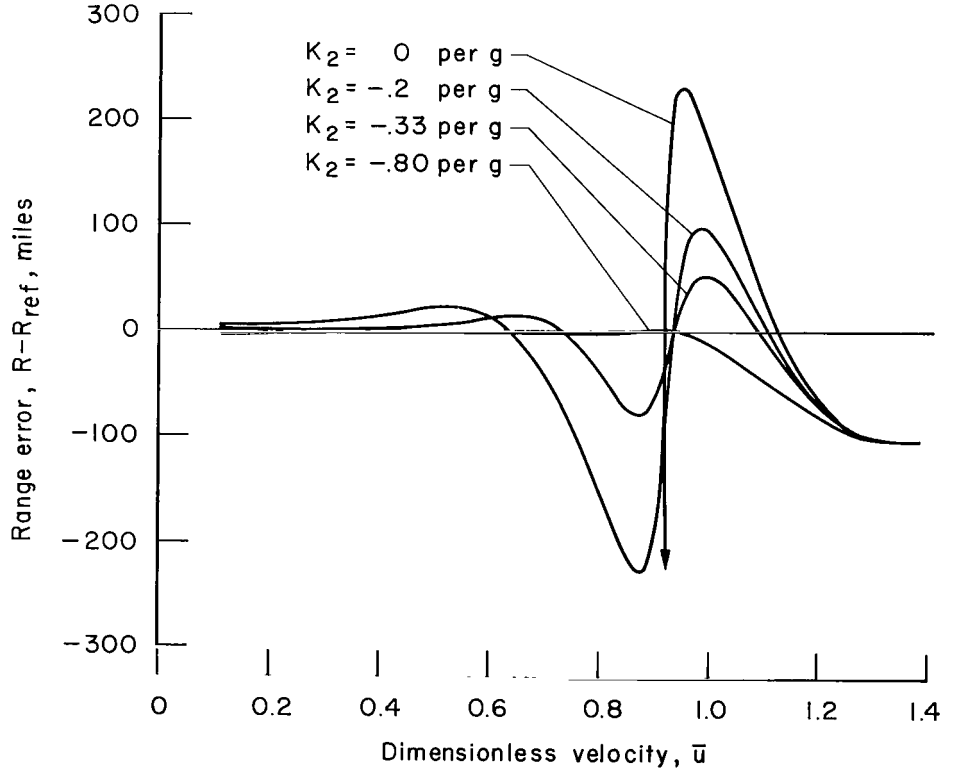

(b) Effect of K_2 with $K_1 = -0.001/fps$.

Figure 16.- Effect of control gains, K_1 and K_2, on range error using range control for trajectory 3 with $K_3 = 0.006/mile$; $\gamma_1 = -4.3^\circ$.

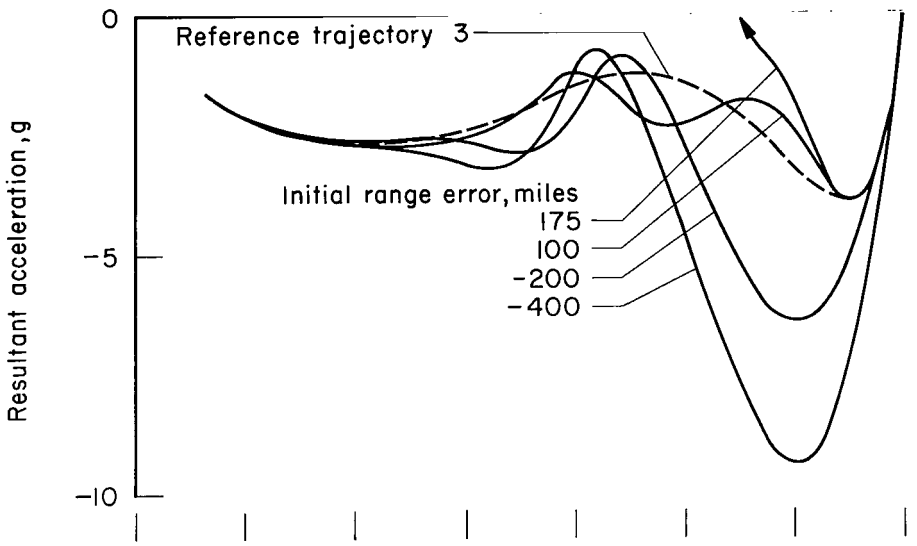

(a) Acceleration

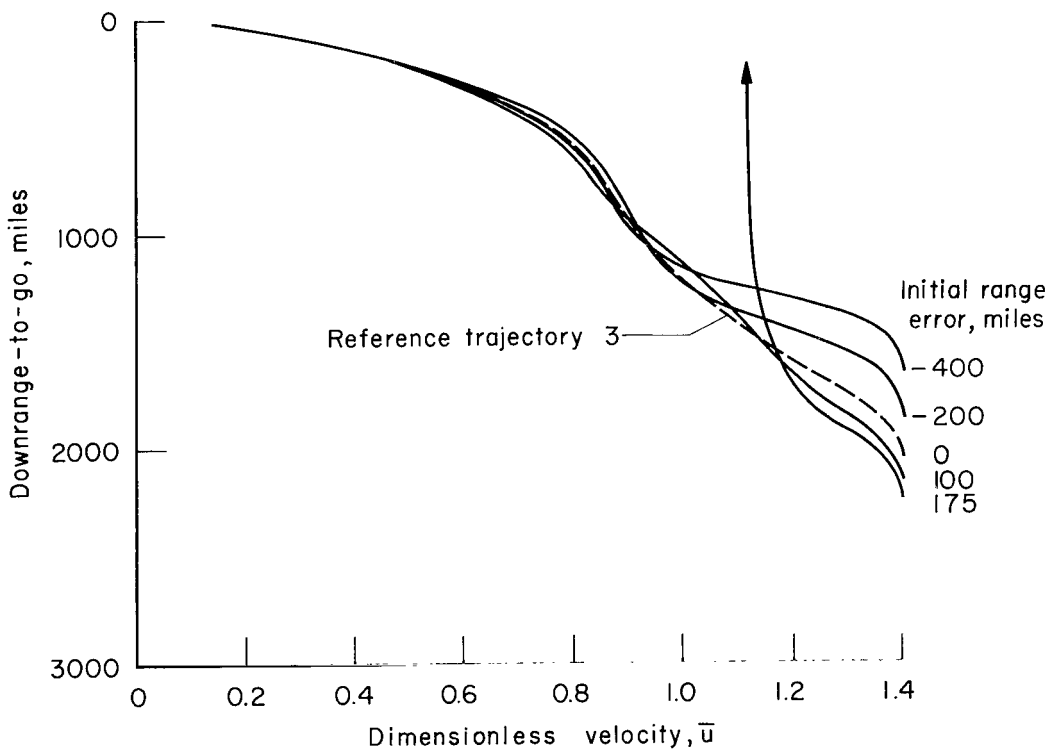

(b) Downrange

Figure 17.- Control to reference trajectory 3 for range control with K_1 = -0.001/fps, K_2 = -0.33/g and K_3 = 0.006/mile; γ_1 = -4.3°.

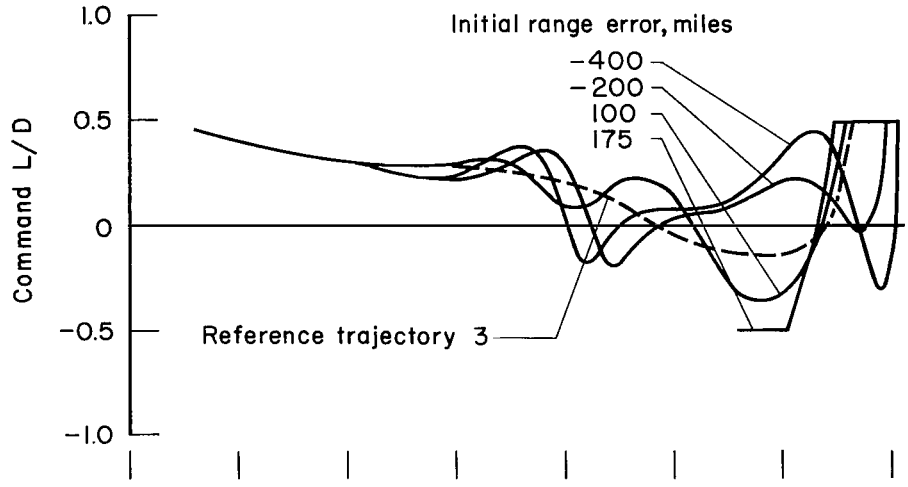

(c) Command L/D.

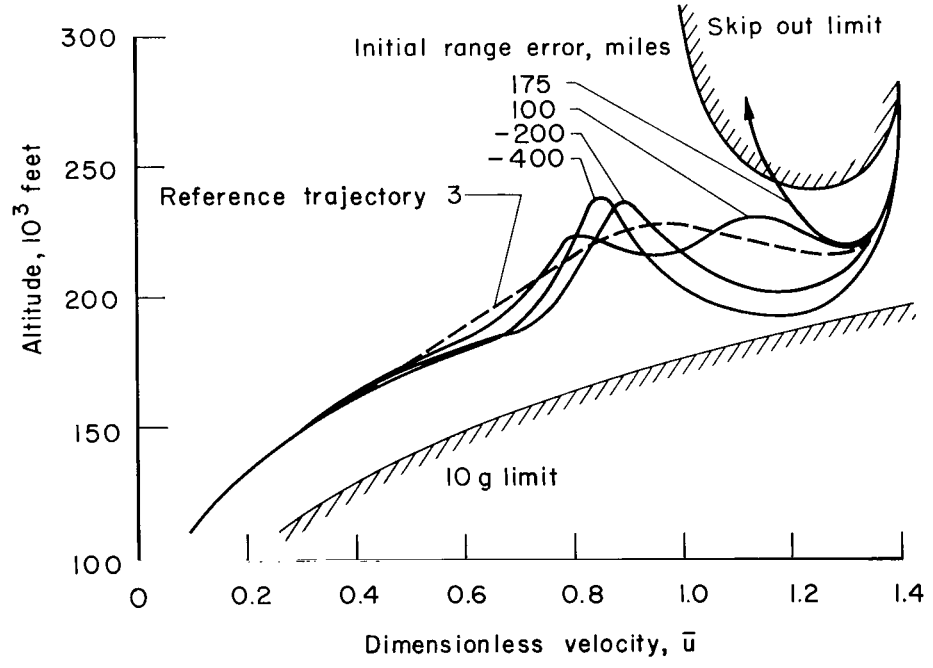

(d) Altitude, W/C_DS = 48 psf.

Figure 17.- Concluded.

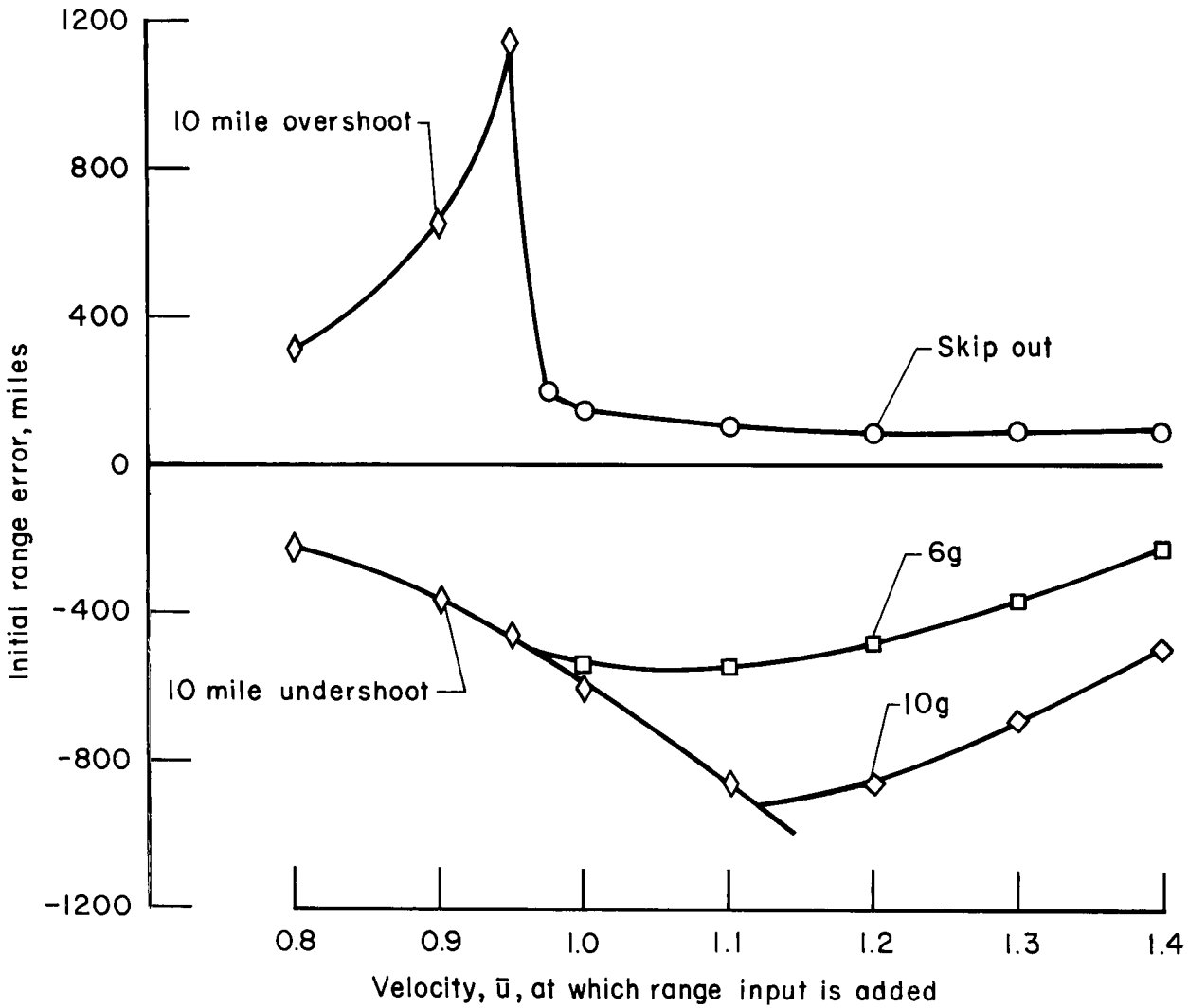

Figure 18.- Initial range error limits as a function of the velocity at which range input is added for trajectory 3 with K_1 = -0.001/fps, K_2 = -0.33/g and K_3 = 0.006/mile; γ_1 = -4.3°.

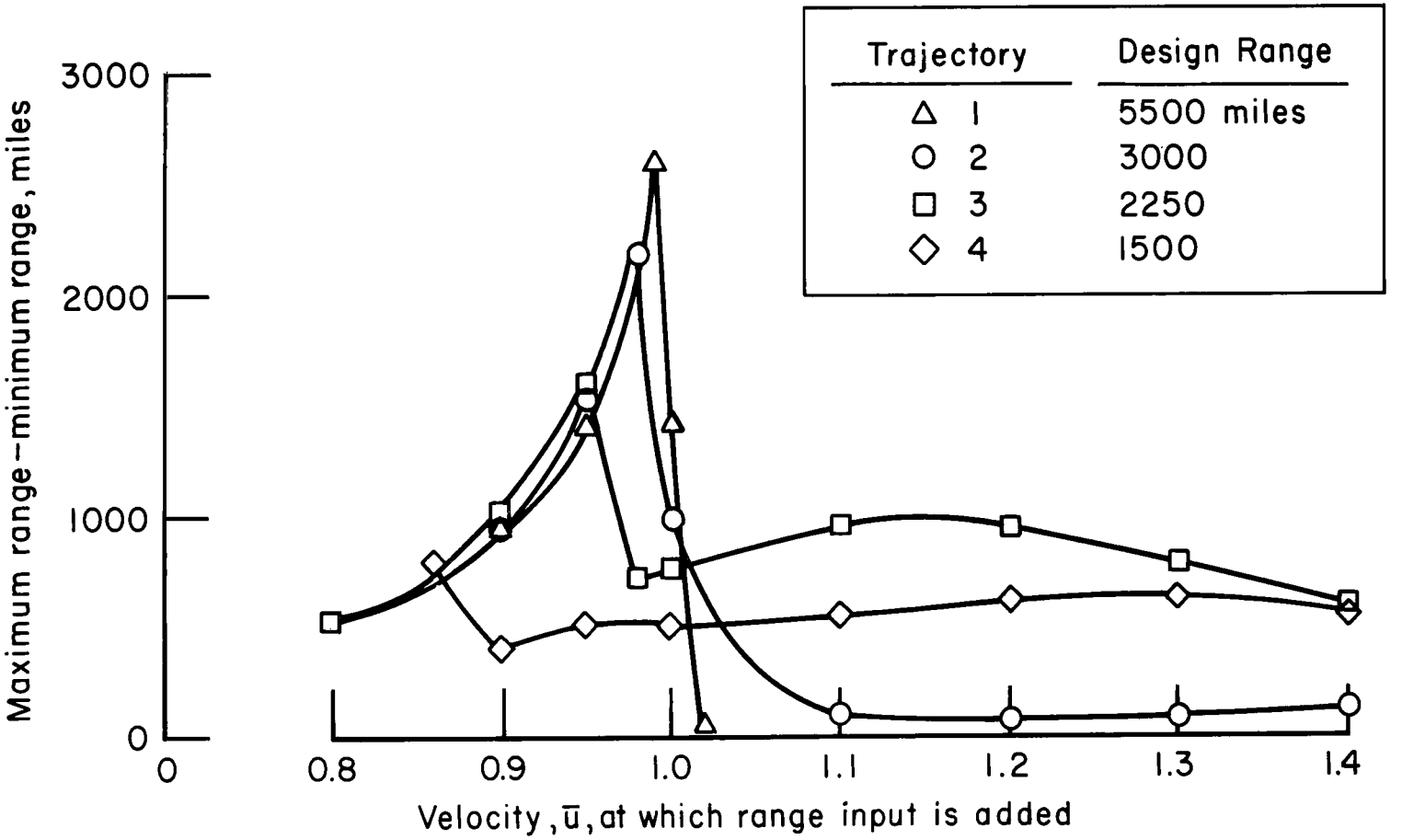

Figure 19.- Range capability as a function of the velocity at which range input is added with K_1 = -0.001/fps, K_2 = -0.33/g and K_3 = 0.006/mile; design γ_1.

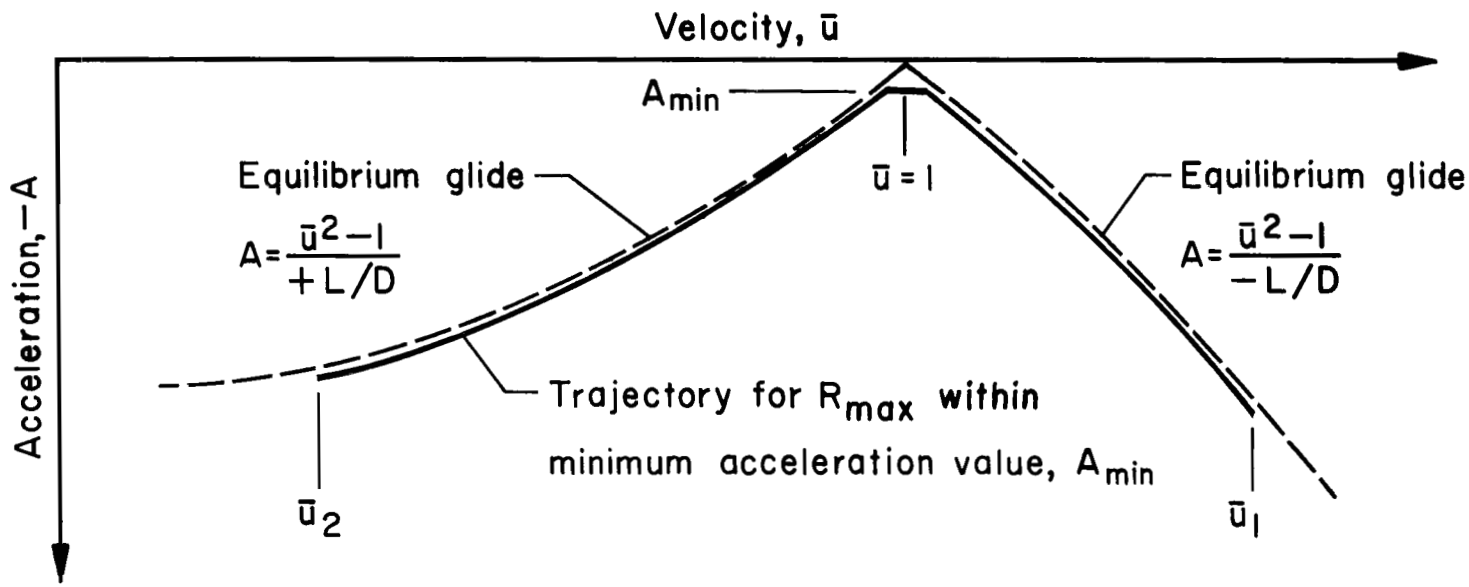

Figure 20.- Approximation to maximum range by the equilibrium glide equation.

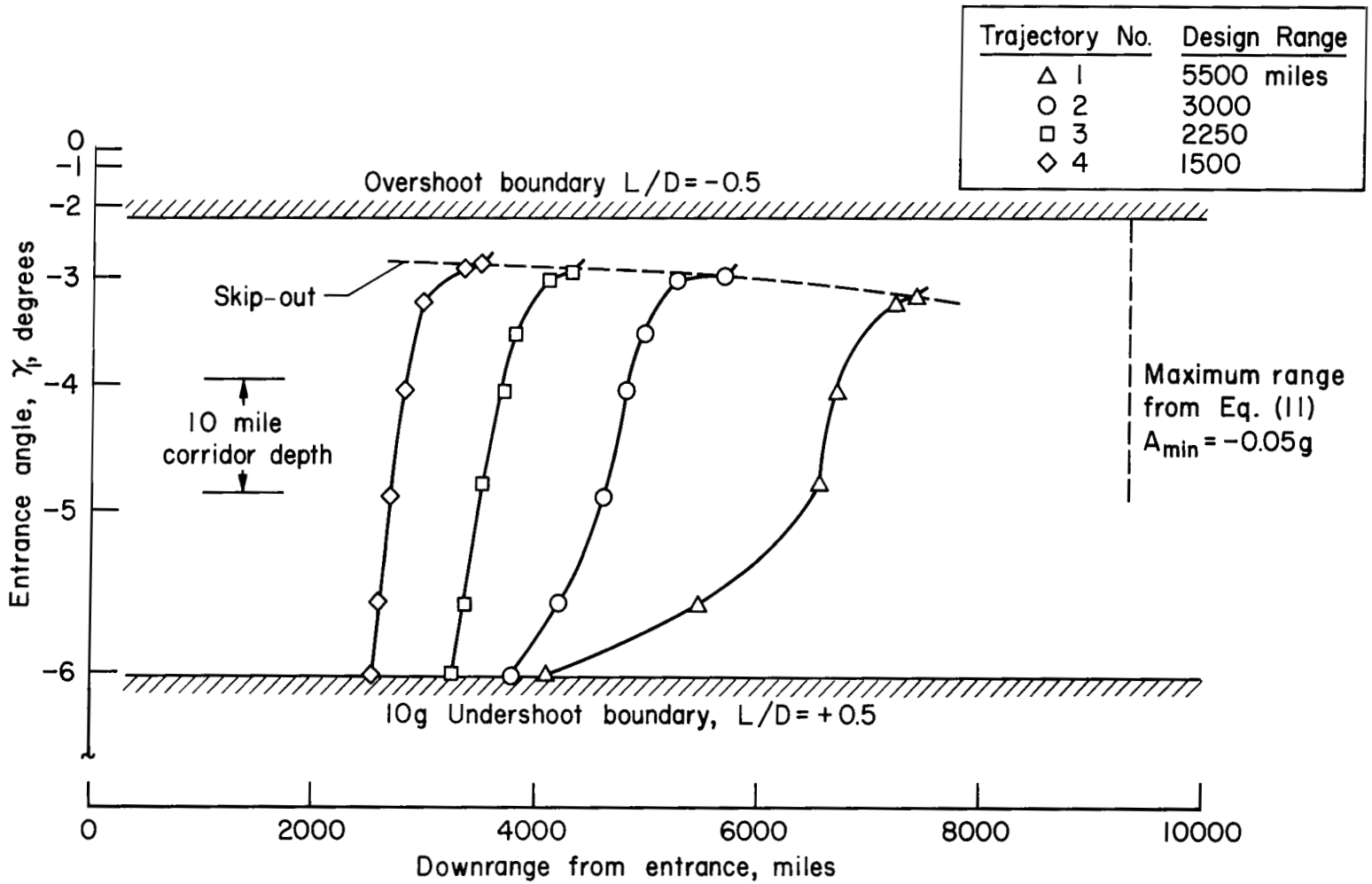

Figure 21.- Maximum downrange as a function of entrance angle using range control with K_1 = -0.001/fps, K_2 = -0.33/g and K_3 = 0.006/mile.

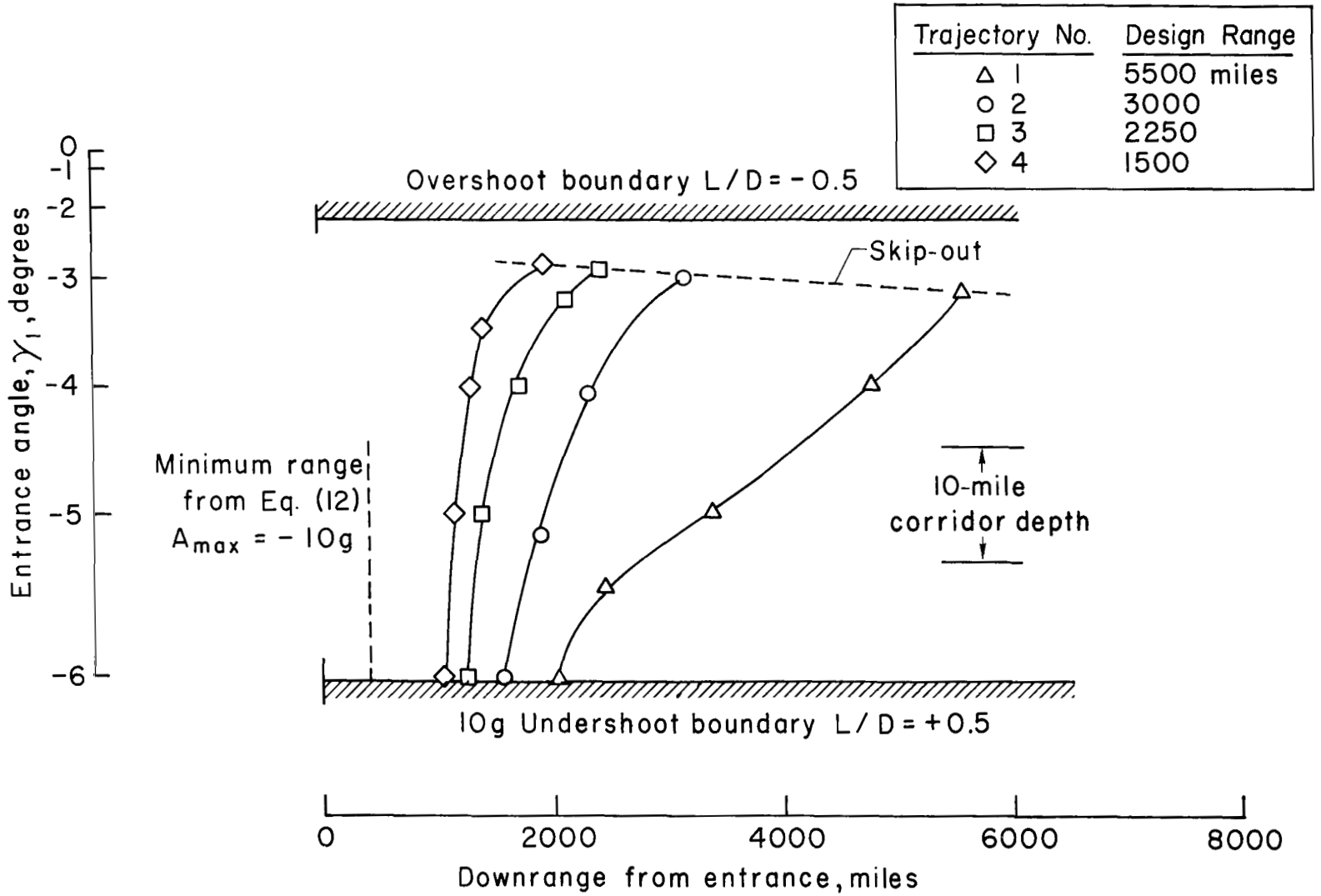

Figure 22.- Minimum downrange as a function of entrance angle for range control with K_1 = -0.001/fps, K_2 = -0.33/g and K_3 = 0.006/mile.

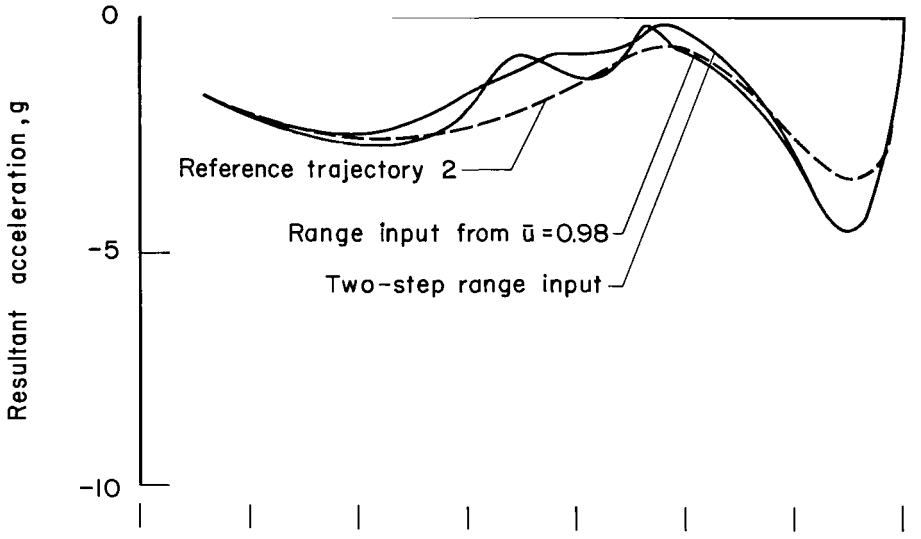

(a) Acceleration

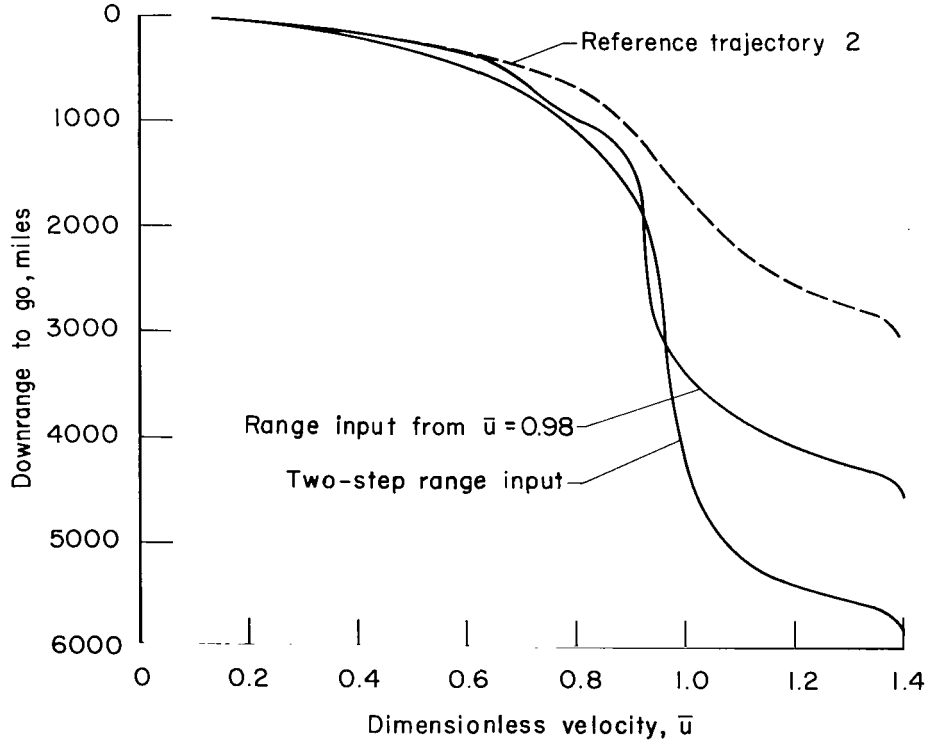

(b) Downrange

Figure 23.- Range control for maximum downrange using trajectory 2 with $K_1 = -0.001/\text{fps}$, $K_2 = -0.33/g$, $K_3 = 0.006/\text{mile}$ and $K_3' = 0.0008/\text{mile}$; $\gamma_1 = -4.5^\circ$.

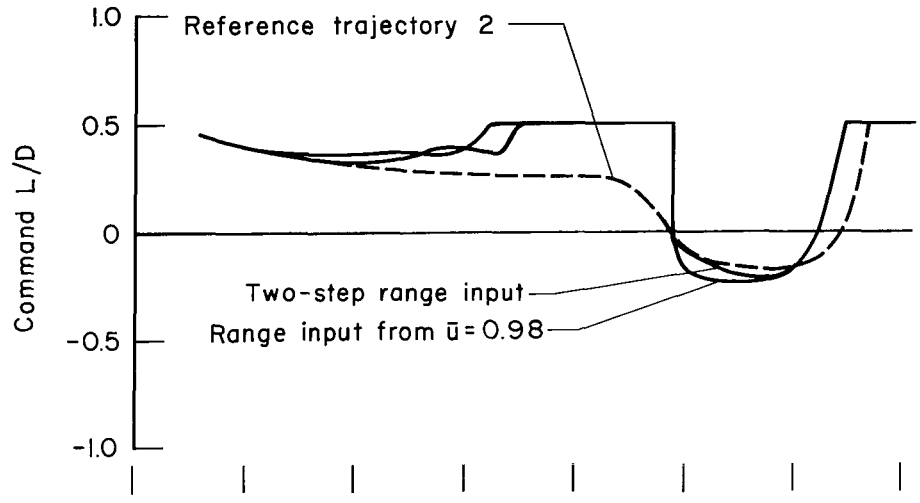

(c) Command L/D.

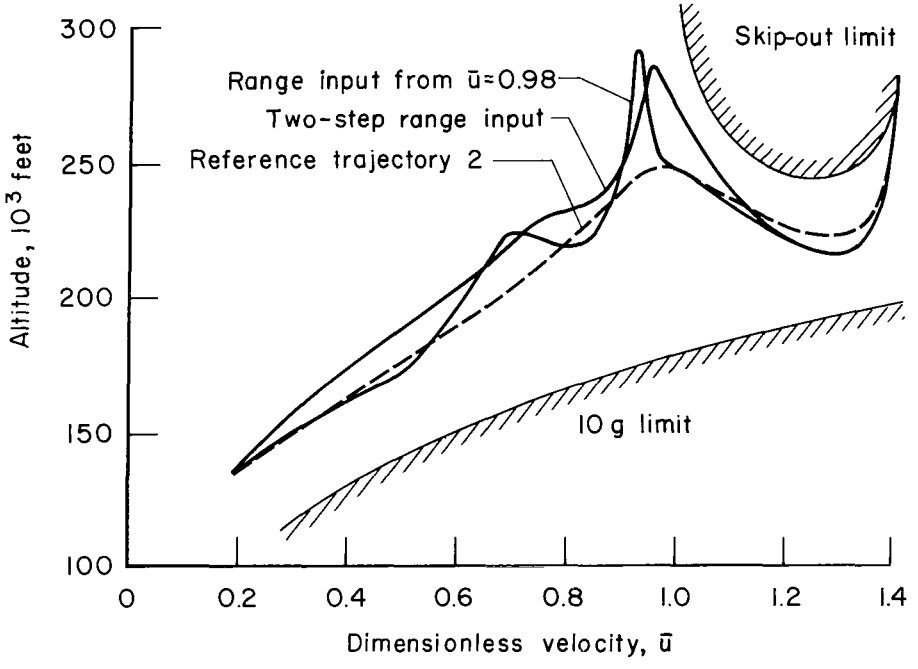

(d) Altitude, W/C_DS = 48 psf.

Figure 23.- Concluded.

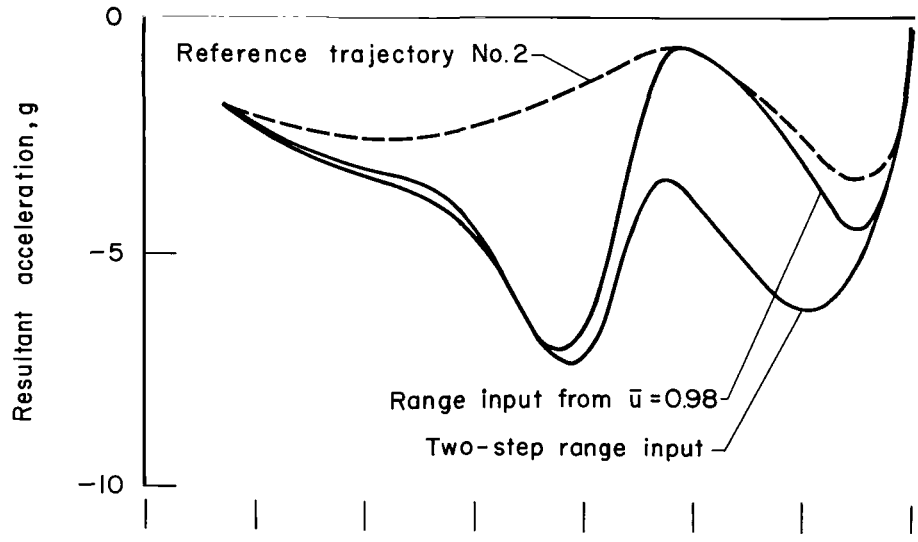

(a) Acceleration

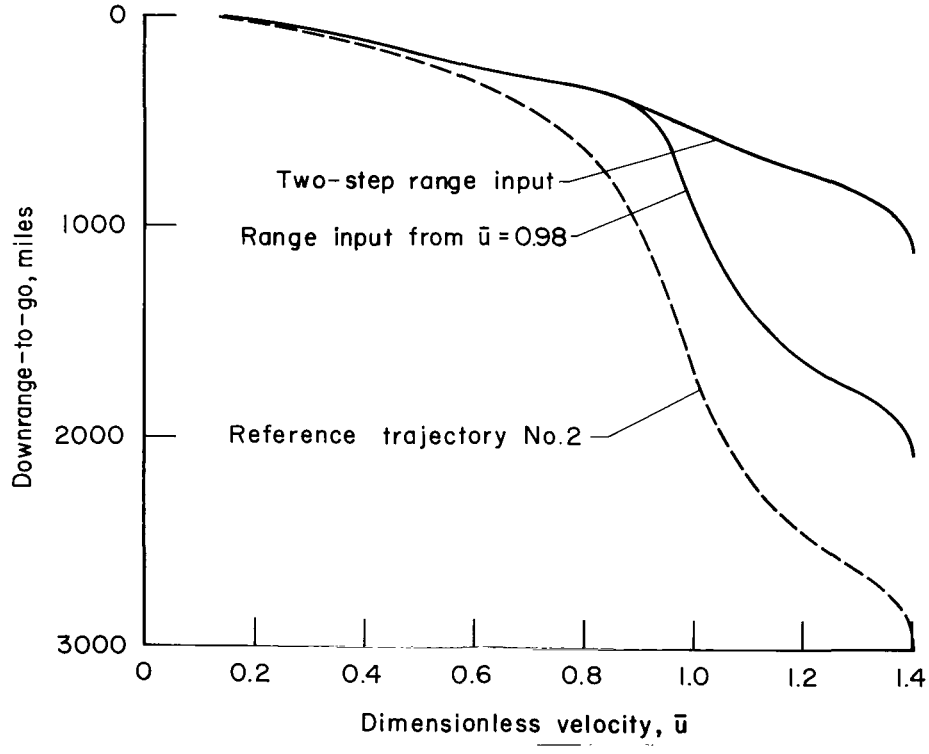

(b) Downrange

Figure 24.- Range control for minimum downrange using trajectory 2 with K_1 = -0.001/fps, K_2 = -0.33/g, K_3 = 0.006/mile and K_3' = 0.0008/mile; γ_1 = -4.5°.

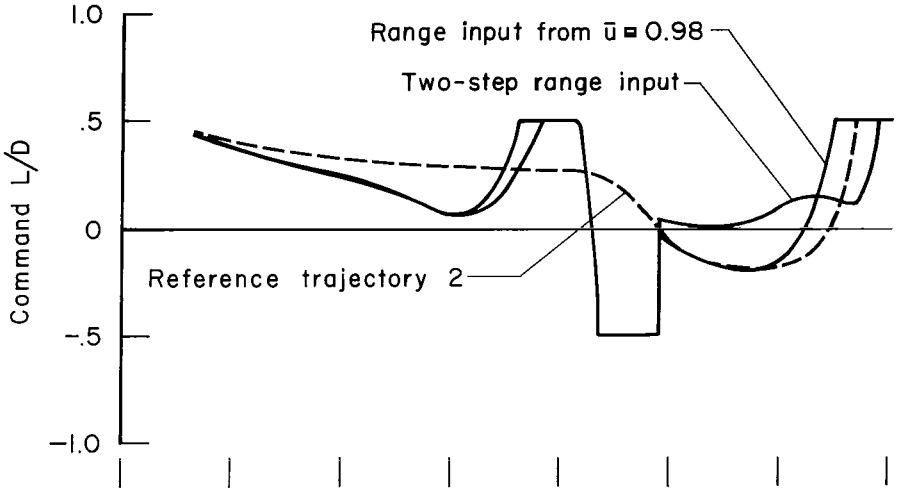

(c) Command L/D.

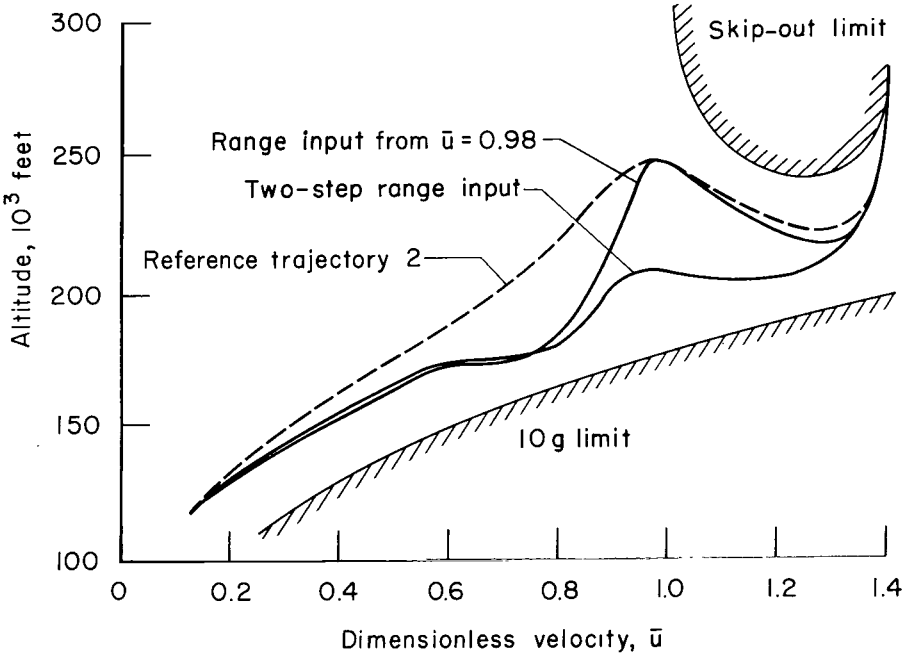

(d) Altitude, W/C_DS = 48 psf.

Figure 24.- Concluded.

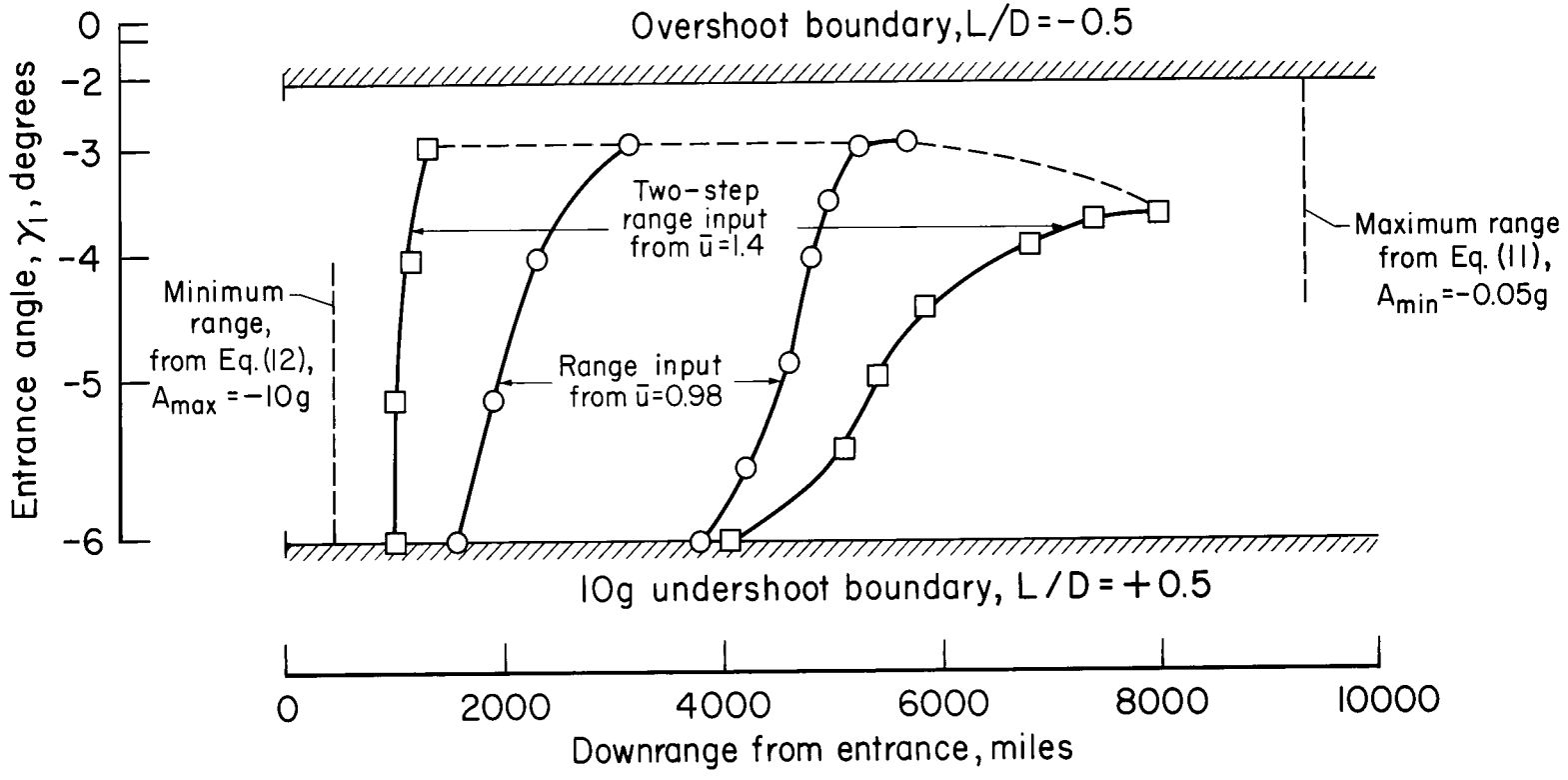

Figure 25.- Downrange capability as a function of entrance angle for trajectory 2 with K_1 = -0.001/fps, K_2 = -0.33/g, K_3 = 0.006/mile and K_3' = 0.0008/mile.

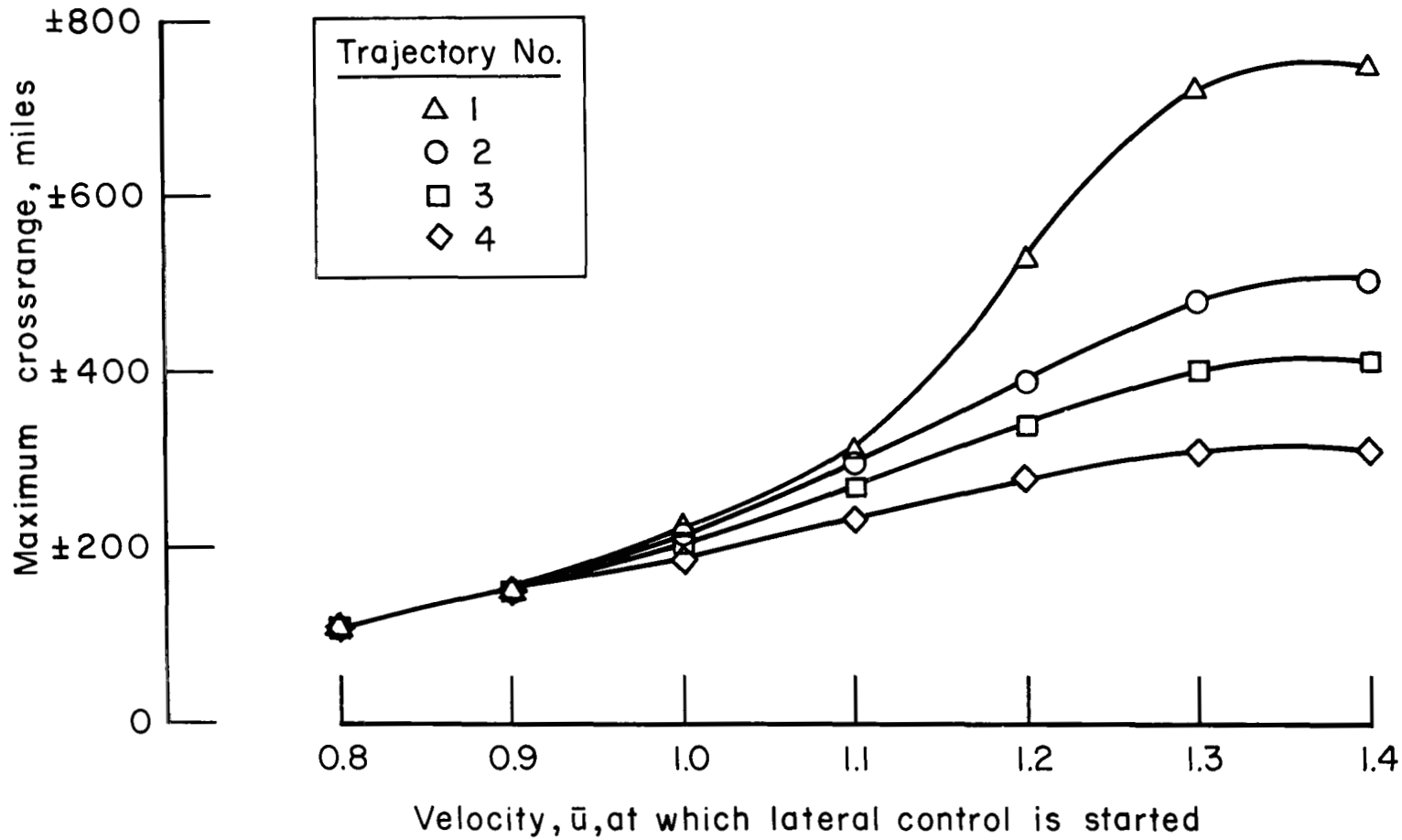

Figure 26.- Maximum crossrange as a function of the velocity at which lateral control is started; design γ_1.

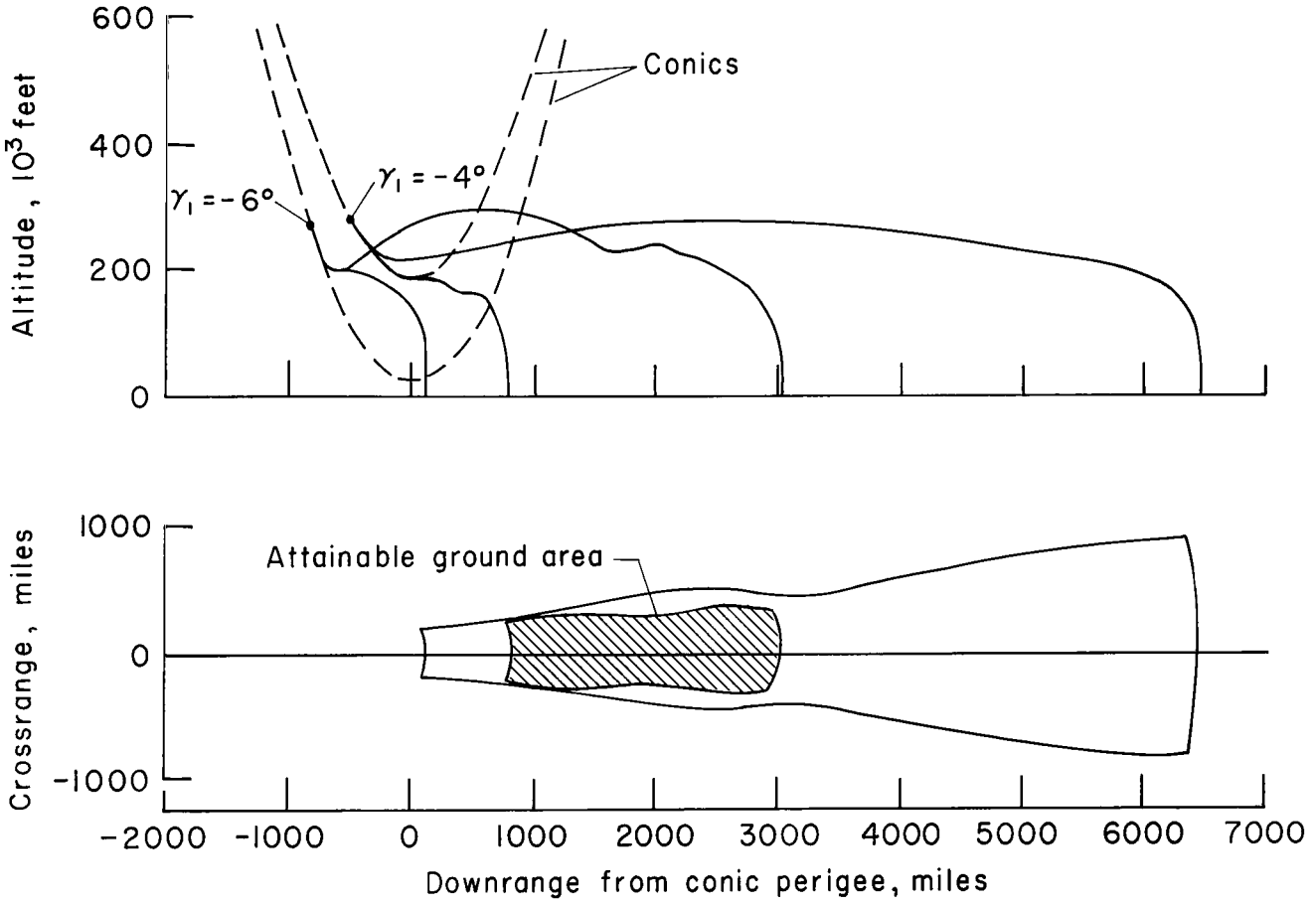

(a) $\gamma_1 = -4°$ and $-6°$, 25-mile usable corridor depth.

Figure 27.- Attainable ground area for various combinations of entrance angles using trajectory 2 with $K_1 = -0.001/\text{fps}$, $K_2 = -0.33/g$, $K_3 = 0.006/\text{mile}$ and $K_3' = 0.0008/\text{mile}$.

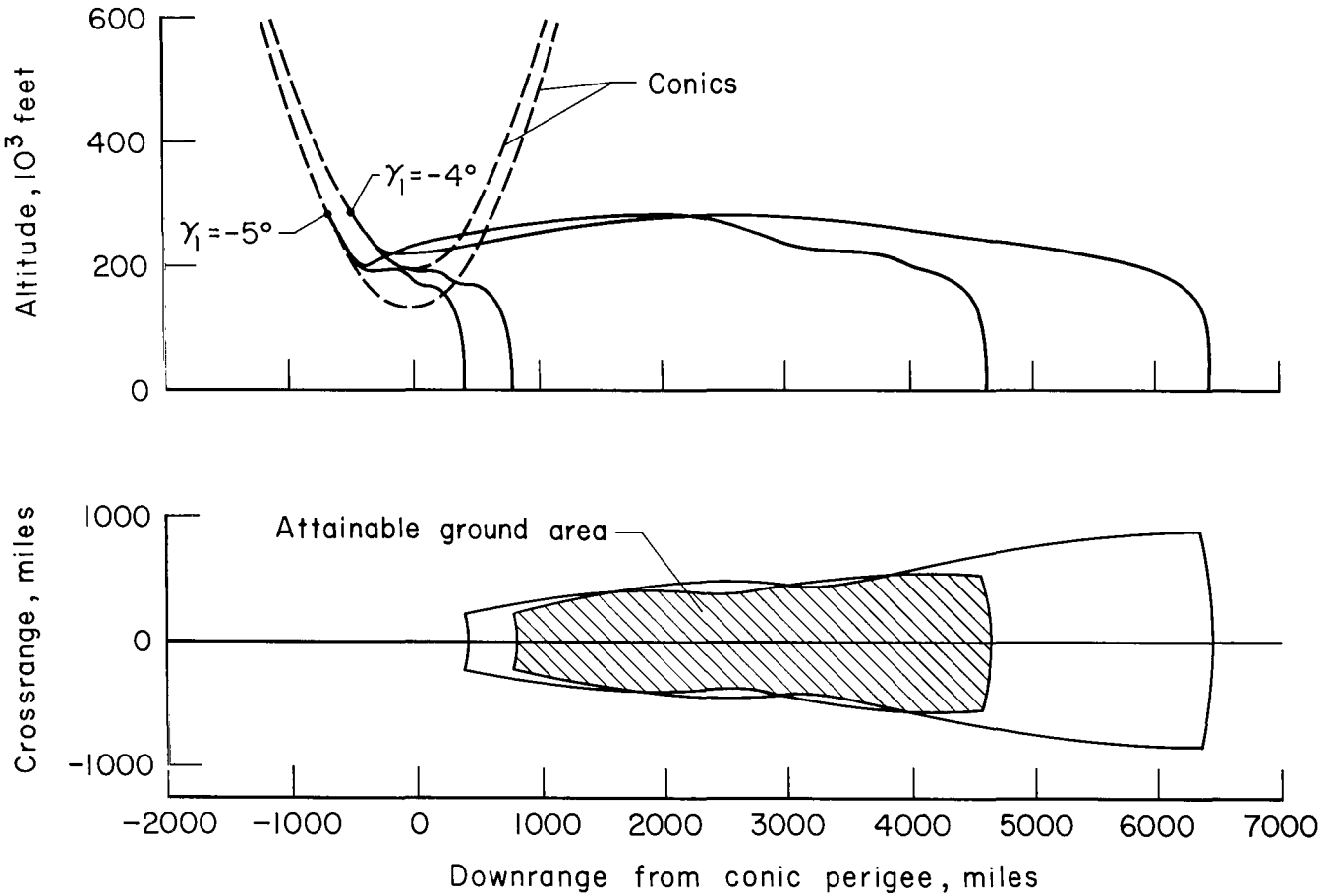

(b) $\gamma_1 = -4^\circ$ and -5°, 11-mile usable corridor depth.

Figure 27.- Concluded.

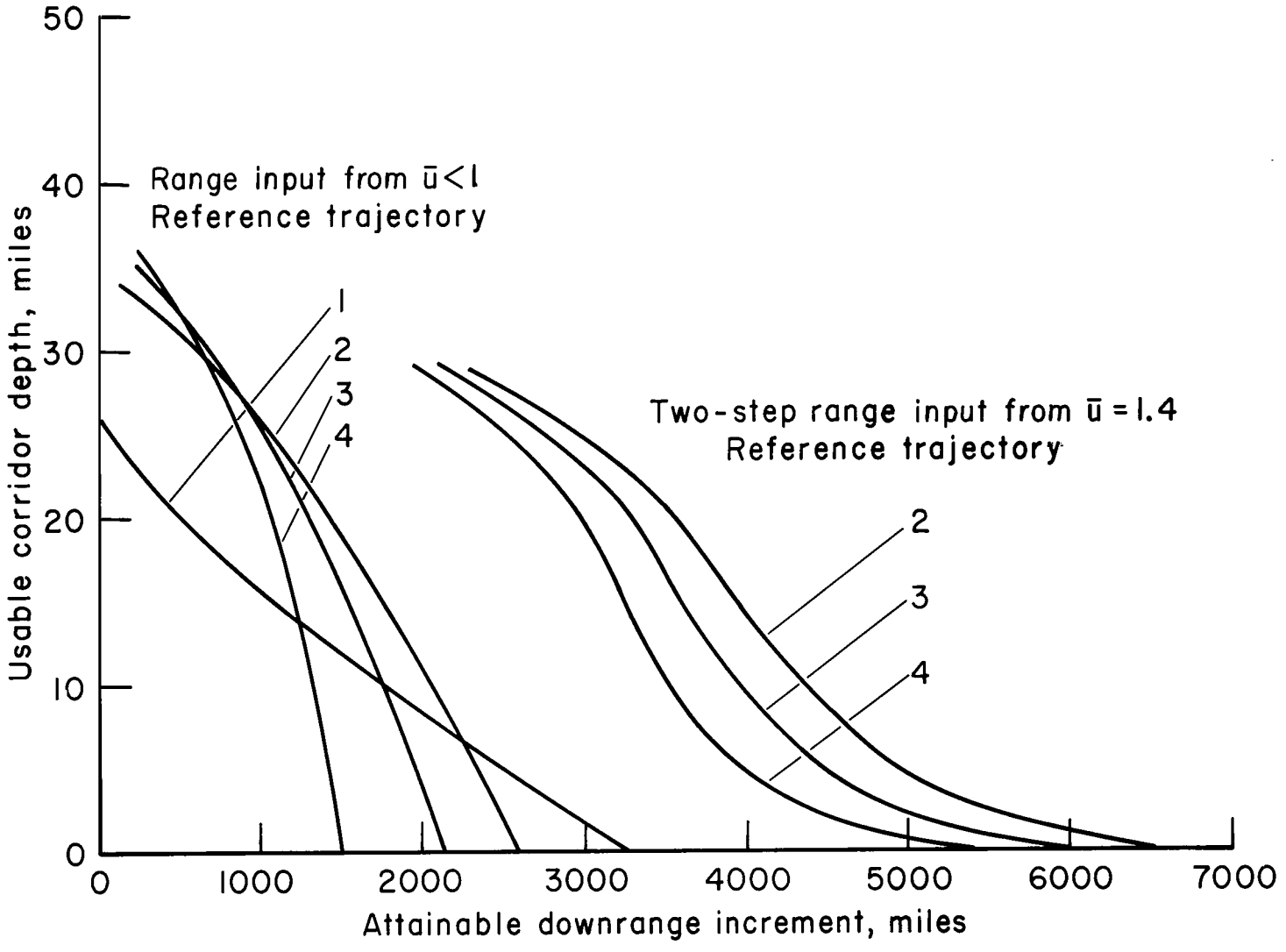

Figure 28.- Attainable downrange increment as a function of usable corridor depth.

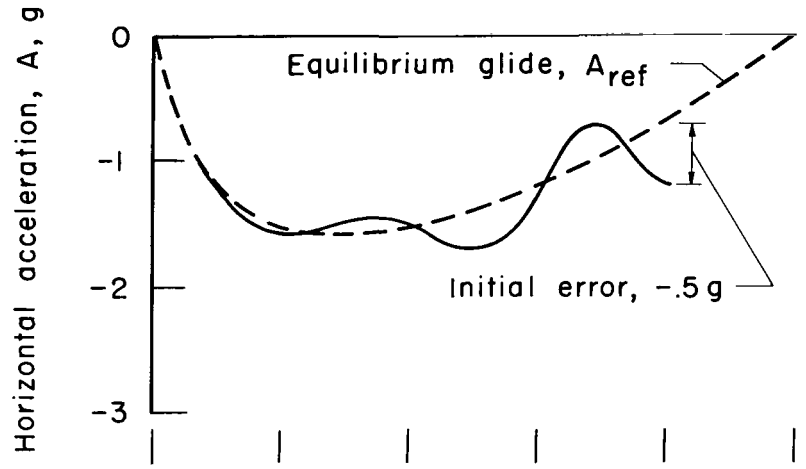

(a) Acceleration

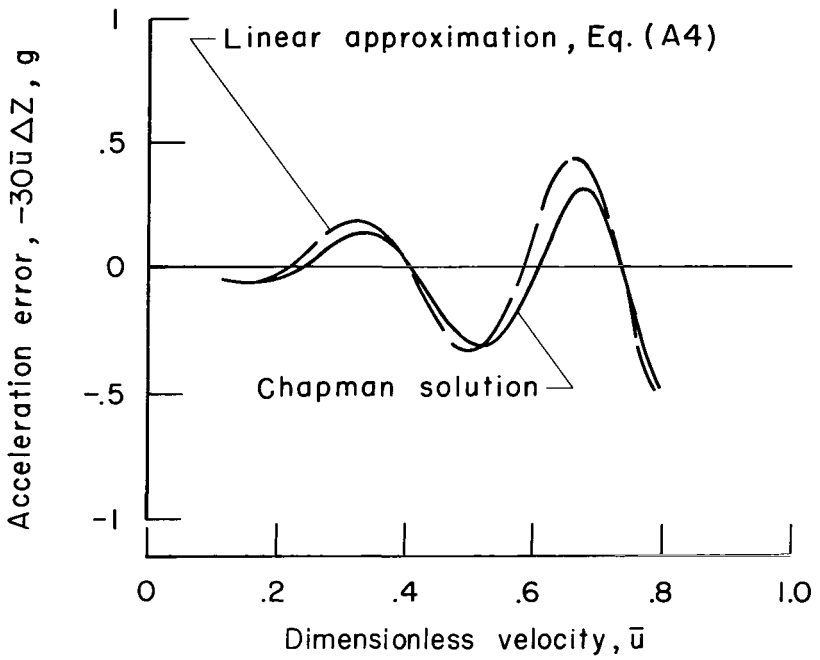

(b) Acceleration error.

Figure 29.- Comparison of a constant L/D = 0.5 trajectory computed by the full Chapman equation compared with the linear approximation; initial conditions, $\bar{u}$ = 0.8, 30 $\bar{u}$ ΔZ = 0.5g, $\Delta Z'$ = 0.

NASA-Langley, 1963 A-683

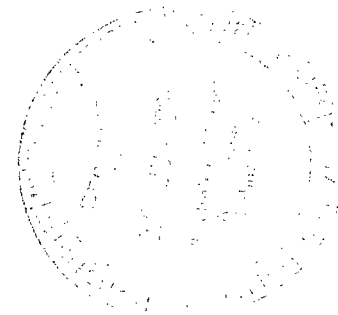

"The aeronautical and space activities of the United States shall be conducted so as to contribute . . . to the expansion of human knowledge of phenomena in the atmosphere and space. The Administration shall provide for the widest practicable and appropriate dissemination of information concerning its activities and the results thereof."

—NATIONAL AERONAUTICS AND SPACE ACT OF 1958

NASA SCIENTIFIC AND TECHNICAL PUBLICATIONS

TECHNICAL REPORTS: Scientific and technical information considered important, complete, and a lasting contribution to existing knowledge.

TECHNICAL NOTES: Information less broad in scope but nevertheless of importance as a contribution to existing knowledge.

TECHNICAL MEMORANDUMS: Information receiving limited distribution because of preliminary data, security classification, or other reasons.

CONTRACTOR REPORTS: Technical information generated in connection with a NASA contract or grant and released under NASA auspices.

TECHNICAL TRANSLATIONS: Information published in a foreign language considered to merit NASA distribution in English.

TECHNICAL REPRINTS: Information derived from NASA activities and initially published in the form of journal articles.

SPECIAL PUBLICATIONS: Information derived from or of value to NASA activities but not necessarily reporting the results of individual NASA-programmed scientific efforts. Publications include conference proceedings, monographs, data compilations, handbooks, sourcebooks, and special bibliographies.

Details on the availability of these publications may be obtained from:

SCIENTIFIC AND TECHNICAL INFORMATION DIVISION

NATIONAL AERONAUTICS AND SPACE ADMINISTRATION

Washington, D.C. 20546